DEGRADABLE MULCH FILMS FOR AGRICULTURAL PURPOSES

A THESIS SUBMITTED TO
THE GRADUATE SCHOOL OF NATURAL AND APPLIED SCIENCES
OF
MIDDLE EAST TECHNICAL UNIVERSITY

BY

ZEKİYE SİSLİ

IN PARTIAL FULFILLMENT OF THE REQUIREMENTS
FOR
THE DEGREE OF MASTER OF SCIENCE
IN
CHEMISTRY

SEPTEMBER 2012

Approval of the thesis:

DEGRADABLE MULCH FILMS FOR AGRICULTURAL PURPOSES

submitted by **ZEKİYE SİSLİ** in partial fulfillment of the requirements for the degree of **Master of Sciences in Chemistry Department, Middle East Technical University** by,

Prof. Dr. Canan ÖZGEN _____
Dean, Graduate School of **Natural and Applied Sciences**

Prof. Dr. İlker ÖZKAN _____
Head of Department, **Chemistry**

Prof. Dr. Ali USANMAZ _____
Supervisor, **Chemistry Dept., METU**

Assist. Prof. Dr.Elif VARGÜN _____
Co-Supervisor, **Chemistry Dept., Muğla Sıtkı Koçman Univsersity**

Examining Committee Members:

Prof. Dr. Teoman TİNÇER _____
Chemistry Dept., METU

Prof. Dr. Ali USANMAZ _____
Chemistry Dept., METU

Prof. Dr. Erdal BAYRAMLI _____
Chemistry Dept., METU

Prof. Dr. Ahmet M. ÖNAL _____
Chemistry Dept., METU

Assist. Prof. Dr.Elif VARGÜN _____
Chemistry Dept., Muğla Sıtkı Koçman Üniversitesi

Date: _____

I hereby declare that all information in this document has been obtained and presented in accordance with academic rules and ethical conduct. I also declare that, as required by these rules and conduct, I have fully cited and referenced all material and results that are not original to this work.

Name, Last name: Zekiye Sisli

Signature:

ABSTRACT

DEGRADABLE MULCH FILMS FOR AGRICULTURAL PURPOSES

Sisli, Zekiye
M.S., Department of Chemistry
Supervisor: Prof. Dr. Ali Usanmaz
Co-supervisor: Assist. Prof. Dr. Elif Vargün

September 2012, 102 Pages

The plastic mulch films, which are mostly made from LDPE, are used in order to increase the yields and to prevent the weed growth by covering the top of the soil by leaves or straw in nature. After a period, the mulch films turn into unmanageable quantities of soiled plastic films, which cause an environmental problem. Using degradable mulch films for agricultural purposes can be a solution for the environmental problems caused by the plastic mulch films.

In this study, to introduce biodegradability to mulch films, a natural biopolymer starch was used. Before blending, starch was transformed into thermoplastic starch in order to make the starch processable. The need, to provide adhesion and interaction between thermoplastic starch and LDPE, citric and stearic acid were considered as compatibilizers. To accelerate the degradation of the LDPE matrix, three pro-oxidants cobalt(II) acetylacetonate, iron(III) stearate and manganase(II) stearate were used.

The films prepared were characterized by FTIR spectroscopy; their thermal and mechanical properties were analyzed and buried under soil. The films recovered from soil after 76 days were characterized by FTIR spectroscopy, their weight loss were measured and their thermal and mechanical properties were analyzed.

Studies showed that the use of cobalt(II) acetylacetonate gave improved results in terms of the mechanical properties and thermal stabilities of the films. Additionally, it is observed that the use of citric acid as a compatibilizer improved the thermal stabilities of starch in the films.

Lastly, it is observed that the mechanical properties of the films were affected by the interactions between compatibilizers and pro-oxidants.

Keywords: Degradation, Mulch film, LDPE, Pro-oxidants, Compatibilizers

ÖZ

ZİRAİ AMAÇLI BOZUNABİLİR MALÇ FİLMLERİ

Sisli, Zekiye
Yüksek Lisans, Kimya Bölümü
Tez Yöneticisi: Prof. Dr. Ali Usanmaz
Ortak Tez Yöneticisi : Yrd.Doç.Dr. Elif Vargün

Eylül 2012, 102 sayfa

Çoğunlukla AYPE'den yapılan plastik malç filmleri, doğada yaprakların ve samanın yaptığına benzer bir şekilde toprağın üstünü örterek verimi arttırmak ve yabani ot oluşumu önlemek amacıyla kullanılmaktadırlar. Bir süre sonra geniş alanlarda kullanılan bu filmler, kontrol edilemez miktarlarda kirlenmiş plastik filmlere dönüşür ve bir çevre problemine yol açarlar. Bu doğrultuda zirai amaçlar için bozunabilir malç filmlerinin kullanımı, plastik malç filmleri tarafından oluşturulan çevre problemlerine çözüm olabilmektedir.

Bu çalışmada, malç filmlerine biyo-çözünebilirlik getirebilmek amacıyla, doğal bir biyopolimer olan nişasta kullanılmıştır. Karıştırılmadan önce nişastayı işlenebilir hale getirebilmek amacıyla, nişasta termoplastik nişastaya çevrilmiştir. İhtiyaç dahilinde termoplastik nişasta ve AYPE arasındaki adhezyonu ve etkileşimi arttırmak amacıyla sitrik ve stearik asit uyumlaştırıcı olarak kullanılmıştır. AYPE matrisinin degradasyonunu hızlandırmak amacıyla kobalt(II) asetilasetonat, demir(III) stearat ve manganez(II) stearat adlı üç farklı pro-oksidant kullanılmıştır.

Hazırlanan filmler FTIR ile karakerize edilmiş olup mekanik ve termal özellikleri analiz edilmiş ve toprağa gömülmüştür. 76 günün sonunda topraktan alınan filmler, bozunmayı gözlemlemek amacıyla, ağırlıkları ölçülmüş, FTIR tarafından karakterize edilmiş, mekanik teste ve termo gravimetrik analize tabi tutulmuştur.

Çalışmalar göstermiştir ki, kobalt(II)asetilasetonat filmlerin mekanik özelliklerini ve termal kararlılıklarını arttırmıştır.İlaveten,uyumlaştırıcı olarak sitrik asit kullanımının filmlerdeki nişastanın termal kararlılığını arttırdığı gözlemlenmiştir.

Son olarak, filmlerin mekanik özelliklerinin, uyumlaştrıcılar ve pro-oksidantların arasında ki etkileşimden etkilendiği gözlemlenmiştir.

Anahtar kelimeler: Bozunma, Malç filmi, AYPE, Pro -oksidant, Uyumlaştırıcı

.

To my father

ACKNOWLEDGEMENT

I would like to present my feelings of gratitude to my supervisor Prof. Dr. Ali Usanmaz for his invaluable guidance, endless patience and support.

I would like to thank to Assist. Prof. Dr. Elif Vargün for her valuable critics and her helps during my study.

I am greatly indebted to Prof. Dr. Teoman Tinçer and Prof. Dr. Erdal Bayramlı for their guidance and providing me every opportunity to use the instruments in their laboratory.

I am very grateful to Zehra Oluz for her help, encouragement, support and friendship. I would like to thank her for spending a lot of time for me and helping me any time I needed throughout this study.

I wish to express my thanks to Sema Zeybel, Seçil Atalay, Yasemin Altun and Talya Yüzücü for their support.

The last but not the least, I would like to present my sincere appreciation to my sister for her support and I would like to specially thank my grandmother for her understanding, help, support and endless love. It would be very difficult to achieve this hard work without feeling their being.

TABLE OF CONTENTS

LIST OF TABLES

TABLES

LIST OF FIGURES

FIGURES

LIST OF SCHEMES

SCHEMES

ABBREVIATIONS

C: Cobalt(II) acetylacetonate

c.a: Citric acid

F: Ferric Stearate

FTIR: Fourier Transform Infrared Spectroscopy

LDPE: Low density Polyethylene

M:Manganese(II)stearate

s.a: Stearic acid

TGA: Thermo gravimetric analysis

TPS: Thermoplastic starch

UV: Ultraviolet

W: Wheat starch

CHAPTER 1

INTRODUCTION

1.1 BACKGROUND INFORMATION

Petrochemical polymers have offered many practical utilities to humankind. However, the ecosystem is fairly affected in a negative way as a result of the non degradable polymers used for disposable items such as plastic bags used for the disposal of the garbage, packaging materials and mulch films. Conventional methods for the disposal of plastic waste material such as burning the items, burial of the bulk waste and cycling are now regarded as inadequate. Moreover, petroleum sources are finite and need to be replaced with a sustainable one. Finding durable alternatives to plastics, for short term disposable applications has become relatively important. The environmental impact caused by persistent plastic waste has resulted in a research interest aiming to replace conventional non degradable polymers with degradable polymers [1,2].

1. 2 MULCH FILMS

By the year 2000, worldwide plastic production exceeded 150 million metric tons per year, with increases expected to continue [3]. Plastic consumption is 1.3 million tonnes in worldwide by 2008. The annual consumption of plastic films for greenhouses (Figure1), low tunnel (Figure2), and mulching (Figure3,4), is about 1.3 million tonnes world-wide [4].

Figure 1: Greenhouse [5]

Figure 2: Low tunnel [6]

Figure 3: Mulch film [7]

Figure 4: Mulch film [8]

Mulching is the practice of covering the top of the soil with a plastic film as has been done by leaves or straw in nature. The plastic mulch films are mostly made from low density polyethylene (LDPE) and its copolymers, linear low density polyethylene (LLDPE) and high density polyethylene (HDPE). The dramatic impact on cultivating practices has been made by mulching films. Vast areas of land are covered by these films in simple and efficient mechanical spreading methods.

The main benefits of mulching films can be listed as; conservation of moisture in soil, increase in the soil temperature, preservation of tilth, weed and pest control and prevention of loss of nutrients and fertilizers applied. All of these factors combine to give improved yields [9].

1.2.1 The disposal problem of mulch films after their use

The mulch films which are spread over large areas have to be collected after the harvest. Repeating this action every 7-8 month period results in unmanageable quantities of soiled plastic films. There are some possible ways in order to get rid of these huge amounts of plastics however they are not efficient. One of the ways to discard the waste is burning the material. However, burning is not permitted in lands by many countries, more important it is hazardous to environment; the smoke of burning plastic contains toxic particles which harm the nature, even then burning plastic melts, chars and becomes a block of material that will resist all further handling.

Another solution is the burial of the waste material, however transportation to landfills is costly and the lack of landfill facilities generally restricts this option. Recycling can be considered as a sustainable solution to this problem. However, mulch films highly contaminated by soil and plant debris are partly oxidized and affected by various agrochemicals are not suitable for recycling.

For the last decades, with the progress of finer raw materials and better manufacturing methods, it is possible to use mulch films with thickness varying between 20-30 microns. Such thin films are easily disintegrated into fragments by the help of external factors. Mulch films are collected after the harvest; however it is not completely possible to collect them efficiently since some of disintegrated parts of mulch films remain in the soil. These fragments left in the soil do not degrade and stay in the soil as macro pollutants.

The perfect solution in order to overcome the drawbacks of the usage of mulching films could be the self destruction of mulch films after a time. Degradable mulch films may offer an economical alternative to manual collection and become a solution for ultimate disposal problem [9].

1.3 POLYMER BLENDS

Polymer blends are defined as in which at least two different polymers are blended together to create a new material with different facilities. Polymer blends can be considered as a new class of polymeric materials that are becoming significantly important. The use of polymer blends offers a way to the production of new materials for a specific use with a satisfactory balance of properties and cost. The main target in polymer blending is the improvement of some particular properties of a given homopolymer by adding another specific polymer [2].

LDPE which is the commonly used material for mulch films and starch which is a biopolymer can be blended in order to give a particular property, degradability to mulch films.

1.3.1 LDPE

Most of the mulch films are used in fields over the world wide is made from LDPE, because of its easy availability, process-ability, flexibility, seal strength and its low cost also favours its use [10].

Low density polyethylene (LDPE) is produced by the high pressure polymerization of ethylene.

It has branching at random places leading to low packing of polymer chains. LDPE is semi crystalline has crystalline and amorphous parts.

Its density varies between 0.910 to 0.925 g/cm^3 and its molecular weight may be up to 4×10^6. LDPE is a thermoplastic polymer which has a melting point between 106-112^0 C. LDPE has a soft and flexible nature as result of its low glass transition temperature. The glass transition temperature of LDPE is between -20^{0}C and -125^{0}C [11].

LDPE has a highly hydrophobic and inert surface. It is a result of having a backbone consisting of long carbon chains consisting of only CH_2 groups [12].

1.3.1.1 Degradation of LDPE

The exposure of polymers to natural outdoor conditions which refers to natural weathering causes the degradation of the materials. The natural elements of outdoor weathering include solar radiation, temperature, oxygen, ozone, moisture, chemical pollutants and bio organisms. The overall degradation can be extremely complex due to the fact that variable factors have a role in the process.

The oxidation of LDPE which is the most important components of the chemical environment, begins during processing, the rate of thermo and photo oxidation of the LDPE through its lifetime is affected by the formation of hydro peroxides during manufacturing [9]. Antioxidants in other words processing stabilizers are used to minimize the mechanoxidation during fabrication.

Despite all these degradative factors since LDPE has high molecular weight and commercial LDPE contains antioxidants and stabilizers, the ultimate degradation of LDPE may take several hundred years [12].

1.3.1.1.1 Abiotic degradation: Precursor to biodegradation

The low molecular weight fragments which can be used as nutrients by micro organisms are mostly produced by the normal abiotic mechanisms of organic and physical chemistry.

The oxidation of the LDPE is observed in the amorphous regions of the polymer since the crystalline regions are impermeable to oxygen. When oxidation takes place, tie molecules get scissioned, causing a decrease of elongation and other physical properties. The destruction of the amorphous regions and tie molecules causes a decrease in mechanical properties of the polymer and leading to the rapid physical disintegration of the whole polymer [2,9].

Photo degradation is a process where the decomposition of the plastic molecules takes place as a result of long exposure to UV light. Oxidation and photo oxidation occur primarily on the surface of the film but the oxidation extends through the bulk after a long time interval. It is reported that when the polymer is exposed to the UV light, it leads to uptake of oxygen, formation of carbonyl, hydroxyl and vinyl groups, evolution of acetone, acetaldehyde, water, carbon monoxide and carbon dioxide, increase in brittleness, generation of crosslinks and mechanical failure of the LDPE [13]. The cleaved chains are mostly ended with the formation of carboxylic groups but esters, ketones, alcohols and double bonds can also be formed [14].

Scheme 1: Degradation of polyethylene [2]

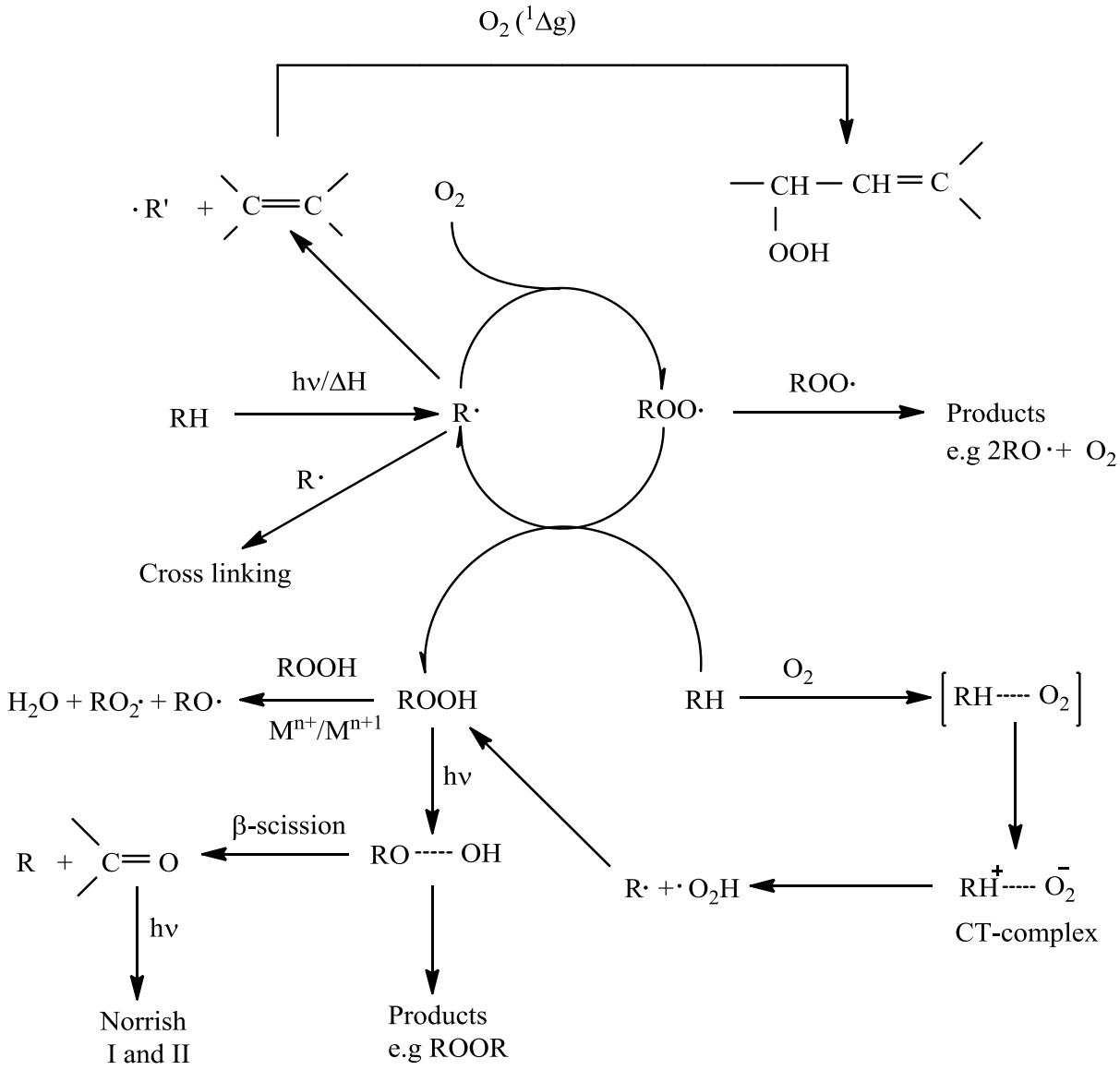

Scheme 1 outlines the possible reactions that can take place during the lifetime of the polymer. Moreover, when the oxygen is absent β – scission by alkyl (R') radicals and cross linking by peroxyl (ROO') radicals takes place to result in unsaturation and insoluble gels.

Represented as M^{n+} and $M^{(n+1)}$ in scheme 1, metallic impurities from catalyst residues in low-pressure polymerization processes and processing equipments can influence the photo oxidation mechanism by catalyzing the ionic decomposition of hydro peroxides [2].

Scheme 2: Norrish type I and Norrish type II reactions [2]

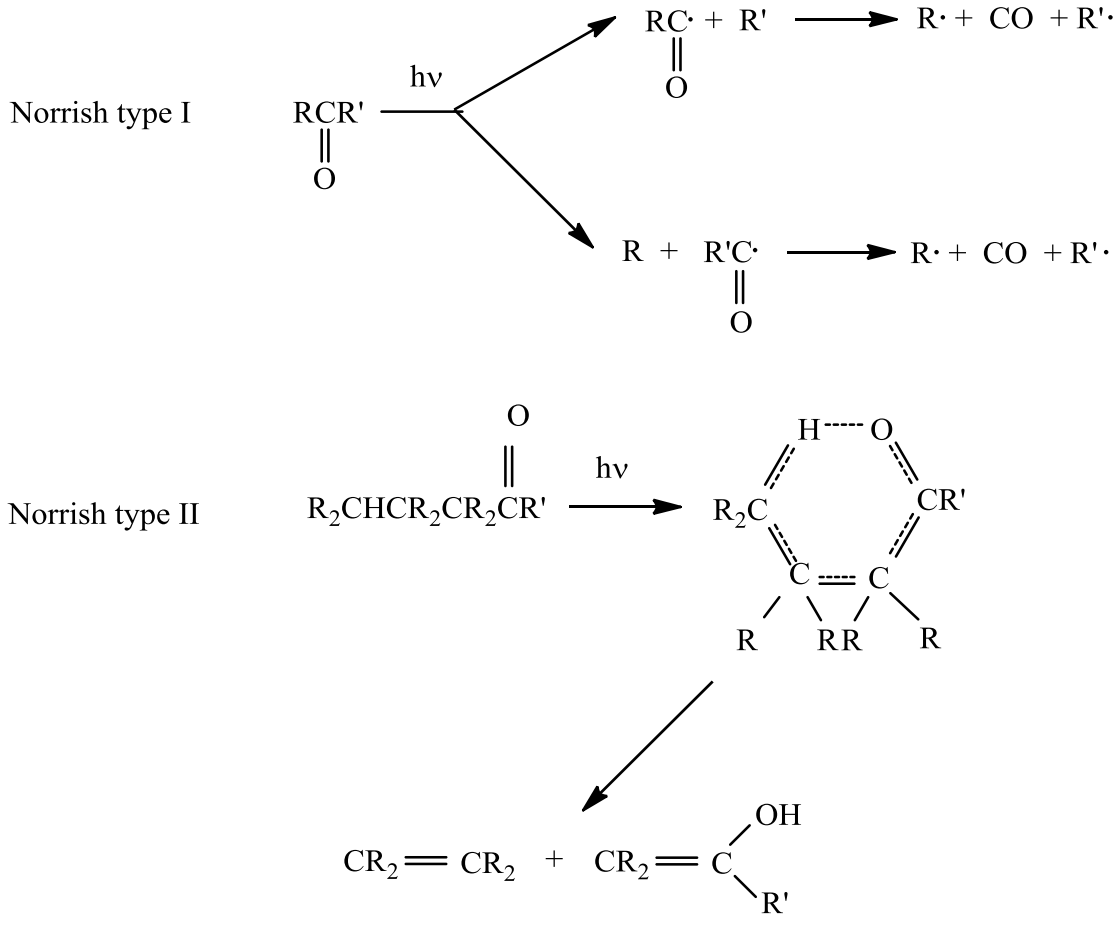

Thermal degradation of polymers can take place in the presence of heat. When the polymer is heated to the extent of bond rupture, LDPE degrade by random scission. This results from the production of free radicals along the backbone of the polymer, which results the macromolecule to be divided into smaller molecules of different chain lengths. When a free radical occurs along the backbone of the polyethylene, chain scission is observed, producing a macromolecule with an unsaturated end and another with a terminal free radical. This free radical can come together with another free radical to form an alkane or take a hydrogen form an adjacent carbon, generate a saturated end with a new radical.

Apart from direct chemical reactions that cause degradation, there are other factors effects the degradation of the polymers. During the service time of the mulch film that are subjected to static or dynamic mechanical stress with weathering. Applied stress can lower the thermal activation energy for bond rupture resulting in acceleration of the generation of radicals [2].

1.3.1.1.2 Biodegradation of LDPE

The breakdown of materials by the action of living organisms is called biodegradation. Biodegradation is a process in which the end results in transformation of organic substances into inorganic products, conversely to the other degradation developments. Mineralisation in other words ultimate degradation refers as the complete degradation [15].

The rate of biodegradation is slower when it is compared to rates of chemical and physical degradation. Biodegradation of LDPE first starts with the attachment of microorganism to the surface of the polymer. Microorganisms can attach to the surface of the polymer if only the surface is hydrophilic. LDPE has just – CH_2 groups in its backbone hence its surface is highly hydrophobic. But physical and chemical degradation leads to insertion of hydrophilic groups on the LDPE backbone and making susceptible for microbial attack. After the attachment of microorganism

to the surface of the polymer, the polymer is used as a carbon source. In the very first step of the degradation process ,as the main chain cleaves, the formation of low molecular weight fragments are observed namely oligomers and monomers [12].

The micro organisms break down the polymer chain by different methods such as biophysical breakdown, biochemical breakdown and direct enzymatic attack depending on the type of microbial populations with various catabolic versatilities and with diverse ability to adapt to different environmental circumstances [15]. The micro organisms may assimilate the small oligomers as it is diffused into the organisms [12].

Biodegradation can take place under aerobic and anaerobic conditions. Aerobic conditions exist in soil or water where oxygen is present and anaerobic degradation happens in sediments or ground water where oxygen is not present. Under aerobic conditions the ultimate products of degradation are CO_2, H_2O and biomass. When anaerobic microorganisms degrade the polymer, the products are CO_2, H_2O, CH_4 and biomass under methanogenic conditions and H_2S, CO_2 and H_2O under sulfidogenic conditions [12].

In this context, environmental conditions choose the group of microorganisms and the degradation pathway Also the additives used with LDPE will change the fate of the polymer in the environment and make it more suitable for the microbial attack since commercial LDPE used can stay for hundreds of years in the environment [12].

1.3.2 STARCH A BIO-BASED POLYMER

Starch have potential to provide a solution to environmental concerns, the mixing of starch win the matrix of LDPE, can cause the degradation of LDPE and may offer an alternative to conventional plastic mulch films.

Starch is a bio based polymer which is cheap, renewable, and a fully biodegradable natural product derived from various botanical sources such as rice, potato, wheat, banana etc..[16,17]

The term bio based material means polymeric materials derived from renewable sources that can be processed to engineer plastic-like materials of desired structural and functional properties for several applications [18].

1.3.2.1 The Structure and the Properties of Starch

Starch is natural polymer composed of almost linear amylose an α-1,4 polymer and amylopectin consisting of short linear α-1, 4 polymer chains linked to each other by α-1, 6 linkages. The minor component of the starch, amylose which is linear have a molecular weight of several hundred thousand. It is shaped in the form of a helix. The major component amylopectin, whose molecular weight is in the order of several millions has chain length is 20-30 glucose units. Native starch has both amorphous and crystalline parts in which the minor component of the starch, amylose is responsible for the former and the major component amylopectin is responsible for the latter [19].

Native starch is in the form of discrete and partially crystalline microscopic granules. These granules are held together by an extended micellar network of associated molecules. [17].

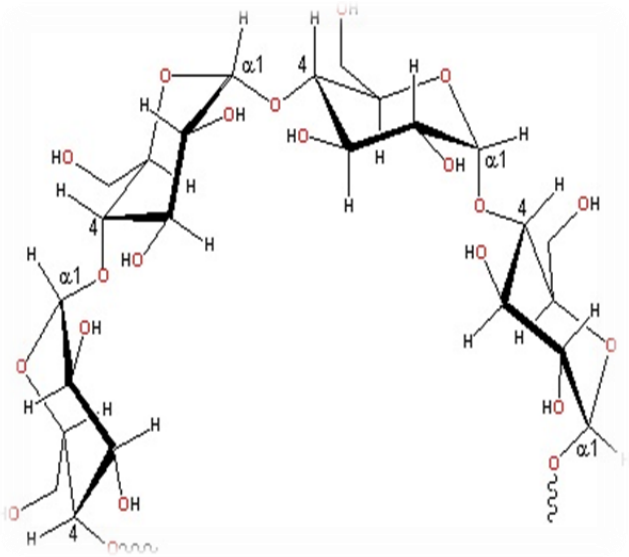

Figure 5: Structure of amylose [20]

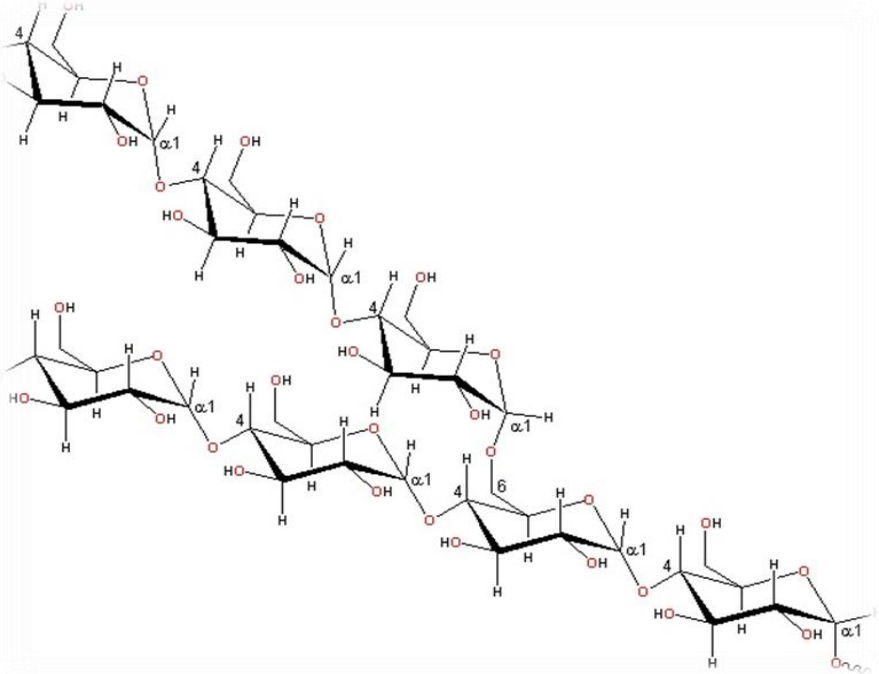

Figure 6: Structure of amylopectin [21]

1.3.2.2 Thermoplastic Starch (TPS)

The dry native starch has processing difficulties depending on its nature, which is composed of separated and partially crystalline granules held together by an extended micellar network of associated molecules [17]. In order to increase the processability of starch, modification of starch is needed. With addition of plasticizer at lower temperatures than degradation temperature of starch under shear and stress, the fusion of mixture of starch granules can be achieved leading to a material composed of entangled polysaccharide chains. This material is called Thermoplastic Starch, (TPS) [22].

Plasticizers play a role in the reduction the intermolecular interactions between the starch molecules by interposing itself between the starch chains and reduce the force holding the chains together. The conversion of native starch which is semi crystalline into homogenous materials with the destruction of hydrogen bonds between the macromolecules is achieved by addition of plasticizers under shear and stress. [23]. Glycerol and water are accepted as one of the most effective plasticizers. These chemicals are small in molecular size and not hazardous to environment [22].

The proportion of plasticizers has a major influence on the physical properties of TPS. The amount of plasticizers added into starch has a influence on the final properties of TPS such as tensile strength, Young's modulus, and glass transition temperature (*Tg*), elongation at break and gas permeability. In addition to this high amount of plasticizers may cause the phase separation. Hence, the amount and the nature of plasticizers have importance in preparation of TPS [23, 24].

Another advantage of converting native starch to TPS is better distribution of starch particles in LDPE. Since TPS shows a better homogenous distribution in the blend, allowing a larger amount of starch to be available to microorganisms resulting in higher rates of biodegradation. A better homogenous distribution also gives better mechanical properties [25].

1.4 COMPATIBILIZERS

Transforming of granular starch into TPS makes the dry starch processable and TPS has a better distribution on LDPE but it is known that LDPE and TPS could form immiscible blends since there is a high interfacial tension between a nonpolar polymer and a highly polar biopolymer [26].

TPS/LDPE blends generally have large phase domains which results in larger non degradable residues and diminished mechanical properties [27]. In order to increase interfacial adhesion strength and bring compatilibility between starch and LDPE, introduction of compatibilizers to these blends can be considered. Hence, to enhance the compatibility between two immiscible polymers, chemicals containing a reactive functional group capable of hydrogen bonding or reacting group with starch hydroxyls can be introduced. In this trend stearic acid and citric acid can be good candidates to have better results for these blends.

1.4.1 Citric Acid

Citric acid can form stable bond interactions with starch and can decrease the shear viscosity and improve the fluidity of TPS. These properties of citric acid increases the dispersion of starch in LDPE and giving better mechanical properties to blends and better biodegradation rates. Citric acid has carboxyl and hydroxyl groups in its structure. These groups of citric acid form strong interactions with the hydroxyl groups in starch and acts as a plasticizer.

The acidity of citric acid promotes the fragmentation and dissolution of the starch granules by disrupting intermolecular and intramolecular hydrogen bonds resulting better distribution of TPS in polymer matrix.

The addition of citric acid enhances the adhesion between citric acid glycerol, water and starch in TPS.

All these improvements achieved by the addition of citric acid as compatabilizer enhances the biodegradation and mechanical properties rates by increasing the distribution of TPS in polymer matrix [26].

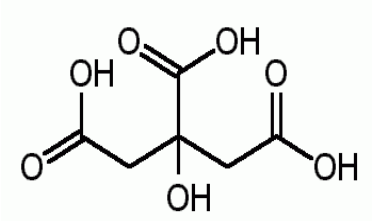

Figure 7: Citric acid [27]

1.4.2 Stearic Acid

Stearic acid can also be a good candidate in order to increase compatibility in starch /LDPE blends. As it can be seen in Figure 10 stearic acid has long alkyl groups and the carboxylic acid group in its structure. Stearic acid act as a compatibilizer due to the fact that its long alkyl group is dispersed in LDPE and the carboxylic acid group interacts with the hydroxyl group starch. .

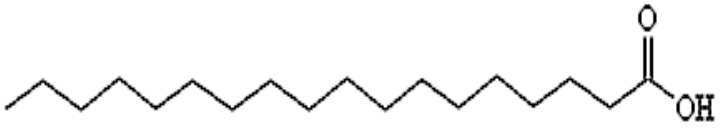

Figure 8: Stearic acid [28]

1.5 PRO OXIDANTS

Despite the fact that UV, heat or oxygen etc cause LDPE to oxidize, adding certain additives is the most effective way in order to increase LDPE chain reactions [30]. Blending starch with LDPE enhances the accessibility of the LDPE to oxygen and microorganisms [31]. In order to accelerate the degradation, the use of some special additives called pro-oxidants can be considered. These chemicals can be the various complexes of transition metals particularly Fe, Co and Mn, typically added in the form of stearate or other organic ligand. These pro-oxidants produce free radicals on the long PE chains; as a result the physical properties of the material lose some of its physical properties. The plastic become oxidized and become more prone to degradation.

Fe^{3+} complex is associated with photo – oxidation process as a source of radicals in order to initiate the reaction [14].

The possible pathway for the mechanism for photo degradation of LDPE in which Ferric stearate plays a role as a pro- oxidant given in Scheme 3;

Scheme 3: The possible pathway for the mechanism of photo degradation of LDPE when Ferric Stearate is used as a pro oxidant [14]

Initiation

Propagation

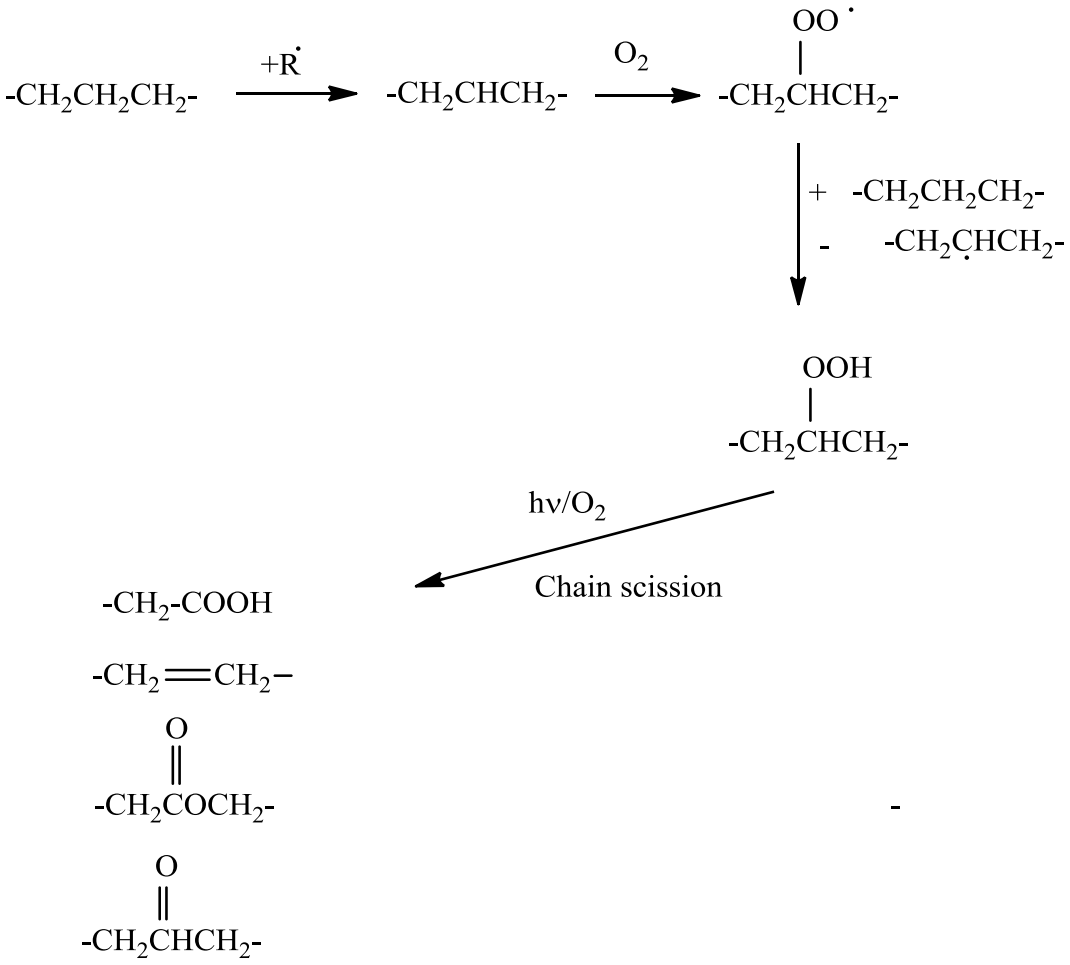

Manganase(II) stearate and cobalt(II) acetylacetonate plays a role in oxidation process without the influence of light . The end products are mostly esters and carboxylic acids [14].

Also pro-oxidants can play a role as compatibilizers due to their structures. The long alkyl groups in the structure of ferric stearate and manganese(II) stearate whose structures are illustrated in Figures 9 and 10, respectively, are dispersed in LDPE and the carbonyl part makes interaction with the starch, resulting in increase in compatibility.

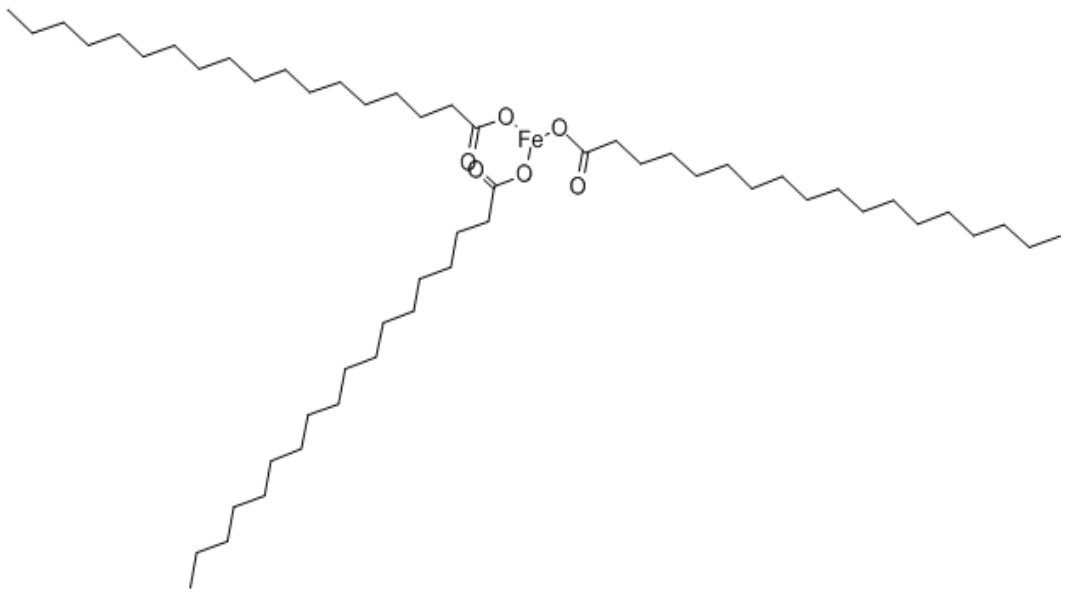

Figure 9: Ferric Stearate [32]

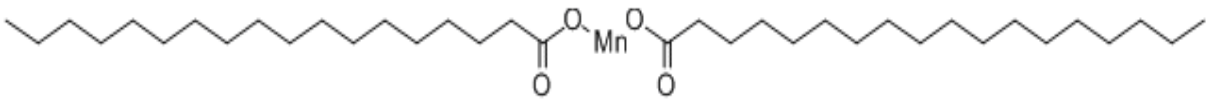

Figure 10: Manganase(II) stearate [33]

Addition of cobalt(II) acetylacetonate the chemical structure is displayed in Figure 11, also may increase the dispersion of TPS on LDPE. The double bond in the structure of the pro oxidant may impart the self plasticizing effect and improves the results.

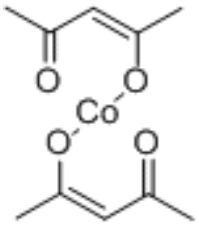

Figure 11: Cobalt(II) acetylacetonate [34]

1.6 AIM OF THE STUDY

Today low density polyethylene is widely used as mulch film in agricultural application causing a source of environmental pollution after their usage. In order to eliminate this problem, changing the conventional film with degradable mulch film can be considered. In this study we have blended starch and LDPE in order to introduce biodegradability to mulch films. Before blending the starch with LDPE, starch is converted to thermoplastic starch to make it processable like a conventional thermoplastic.

The need, to provide adhesion and interaction between TPS and LDPE, citric acid and stearic acid is considered as compatibilizers. By adding these chemicals into blends we aimed to improve the rate of biodegradation and mechanical properties.

In order to accelerate the degradation of the LDPE matrix, pro-oxidants which are the transition metals are added.

Also the interaction between compatibilizers and pro-oxidants are investigated.

CHAPTER 2

EXPERIMENTAL

2.1 MATERIALS

2.1.1 Low Density Polyethylene (LDPE)

LDPE was purchased from Turkish Petrochemical Industry, PETKIM. It was a F2-12 grade.
Some of the selected properties of the polymer are given below:

Melt flow rate (190°C, 2160g): 2.0 - 3.0

Density, 23^0C: 0.920

Melting point: 110^0C

2.1.2 Starch

Wheat starch was obtained from Sigma-Aldrich.

2.1.3 Cobalt(II) acetylacetonate

Cobalt(II) acetylacetonate with 97% purity is provided from Sigma-Aldrich.

2.1.4 Iron(III) stearate

Ferric stearate was purchased from MP Biomedicals.

2.1.5 Manganese(II) stearate

Manganese (II) stearate with 90% purity was purchased from Santa Cruz Chemicals.

2.1.5 Glycerol

Reagent grade glycerol with purity 99.5% was purchased from Sigma Aldrich.

2.1.6 Stearic acid

Stearic acid with purity 95% is purchased from Sigma Aldrich.

2.1.7 Citric acid

Citric acid with purity 99% is provided from Sigma Aldrich.

2.2 SAMPLE PREPARATION

2.2.1 Preparation of Thermoplastic Starch (TPS)

Prior to processing 48% wheat starch 33%, glycerol and 19% de-ionized water by weight were mixed for 10 minutes by mechanical stirrer at 900 rpm. The mixture was then left to stand for 1 hour to allow the starch granules to swell. The starch/glycerol /water suspension was heated for 8-10 minutes at 70^{o}C -75^{o}C. In order to remove moisture from the TPS, it was dried at 60^{o}C in vacuum oven for 48 hours.

2.2.2 Addition of pro-oxidants and compatibilizers

Sample preparation was carried out with three different proxidants, cobalt(II)acetyl acetonate, iron(III) stearate and manganese(II) stearate.

Stearic acid and citric acid were used to increase interfacial adhesion between TPS and LDPE.

2.2.3 Preparation of compositions

Three different types of pro-oxidant, two types of compatibilizers and three different concentrations of TPS were used in this study.

The compositions contain 20 %, 30 %, and % 40 % of TPS by weight according to total weight of LDPE and TPS. Each composition contains one type of pro-oxidant and the amount of pro-oxidant in each composition equals to 0.5% according to total weight LDPE and TPS.

Selected compositions contain 2% of compatibilizers (stearic acid or citric acid) by weight according to total weight of LDPE and TPS. All compositions named in the basis of the type of pro–oxidant used and are shown in Tables 1,2,3 and 4;

Table 1: Compositions for group I: Cobalt (II) acetylacetonate group

Code	TPS + LDPE		Compatibilizer		Pro-oxidant		
	TPS	LDPE	Citric Acid	Stearic acid	Cobalt(II) acetylacetonate	Ferric stearate	Manganase (II)stearate
W20C	20%	80%	-	-	0.5%	-	-
W20Cc.a	20%	80%	2%	-	0.5%	-	-
W20Cs.a	20%	80%	-	2%	0.5%	-	-
W30C	30%	70%	-	-	0.5%	-	-
W30Cc.a	30%	70%	2%	-	0.5%	-	-
W30Cs.a	30%	70%	-	2%	0.5%	-	-
W40C	40%	60%	-	-	0.5%	-	-
W40Cc.a	40%	60%	2%	-	0.5%	-	-
W40Cs.a	40%	60%	-	2%	0.5%	-	-

Table 2: Compositions for group II: Iron(III) stearate group

Code	TPS + LDPE		Compatibilizer		Pro-oxidant		
	TPS	LDPE	Citric acid	Stearic acid	Cobalt(II) acetylacetonate	Ferric stearate	Manganase (II)stearate
W20F	20%	80%	-	-	-	0.5%	-
W20Fc.a	20%	80%	2%	-	-	0.5%	-
W20Fs.a	20%	80%	-	2%	-	0.5%	-
W30F	30%	70%	-	-	-	0.5%	-
W30Fc.a	30%	70%	2%	-	-	0.5%	-
W30Fs.a	30%	70%	-	2%	-	0.5%	-
W40F	40%	60%	-	-	-	0.5%	-
W40Fc.a	40%	60%	2%	-	-	0.5%	-
W40Fs.a	40%	60%	-	2%	-	0.5%	-

Table 3: Compositions for group III: Manganase (II)stearate Group

Code	TPS + LDPE		Compatibilizer		Pro-oxidant		
	TPS	LDPE	Citric acid	Stearic acid	Cobalt(II) acetylacetonate	Ferric stearate	Manganase (II)stearate
W20M	20%	80%	-	-	-	-	0.5%
W20Mc.a	20%	80%	2%	-	-	-	0.5%
W20Ms.a	20%	80%	-	2%	-	-	0.5%
W30M	30%	70%	-	-	-	-	0.5%
W30M c.a	30%	70%	2%	-	-	-	0.5%
W30M s.a	30%	70%	-	2%	-	-	0.5%
W40M	40%	60%	-	-	-	-	0.5%
W40Mc.a	40%	60%	2%	-	-	-	0.5%
W40Ms.a	40%	60%	-	2%	-	-	0.5%

A control group is prepared composed of three samples, containing 20%, 30% and 40 % of TPS without pro –oxidants and compatabilizers in order to see the effects of these chemicals' influence on mechanical properties and degradation rates of the samples.

Table 4: Compositions for contol group

Code	TPS + LDPE		Compatibilizer		Pro-oxidant		
	TPS	LDPE	Citric acid	Stearic acid	Cobalt(II) acetylacetonate	Ferric Stearate	Manganase (II)stearate
W20	20%	80%	-	-	-	-	-
W30	20%	80%	-	-	-	-	-
W40	20%	80%	-	-	-	-	-

2.3 SAMPLE PROCESSING

2.3.1 Extrusion

DSMxplore Netherlands,micro 15cc twin screw compounder was used for the preparation of the blends. Temperature of the three zones were 145^0C - 150^0C - 145^0C . The screw speed was kept at 100rpm, the die temperature was 138 ^{0}C.

2.3.1 Compression Moulding

The blends were compression moulded in Pneumo Hydraulic Press at 150^0C for 4 minutes and the films prepared are stored at 4 ^{0}C for further investigation.

2.4 CHARACTERIZATION

2.4.1 FTIR Spectroscopy

BRUKER VERTEX 70 model FT-IR Spectroscopy is used in this study. FTIR spectra of all samples were recorded by using ATR technique with a resolution of 16 cm^{-1} in a spectral range of 4000–600cm^{-1} using number of 32 scans per sample. The FTIR spectra of the samples were recorded after and before soil burial treatment.

2.4.2 Thermo Gravimetric Analysis (TGA)

Perkin-Elmer, Pyris model Thermo gravimetric analyser is used in this study. The thermal gravimetric analysis of samples was carried out in the nitrogen atmosphere at heating rate of 10^{o}C/min from 25^{o}C up to 600^{o}C.

2.4.3 Tensile Testing

Tensile strength and percentage strain were measured by LLYOD LR 5K at room temperature with crosshead speed of 50 mm/min. Six specimens were tested for each blend. The thicknesses of the films were 100 microns. The mechanical properties of the films were measured before and after soil burial.

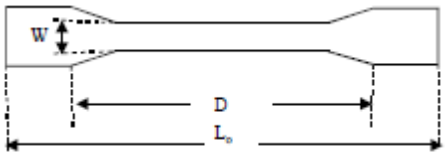

Figure 12: Tensile test specimen

Table 5: Dimensions of the tensile test specimen

Symbol	**Specimen Dimensions (mm)**
W, Width of narrow section	3
D, Distance between grips	30
L0, Total length of specimen	50

2.5 SOIL BURIAL

The plastic box having approximate dimensions 25cm x 19cm x 33cm were filled with the soil with pH 7 obtained from ODTU/ANKARA.

The blended film samples were cut into pieces with dimensions 6cm x 7cm and buried in soil at the depth of 8 cm as it is illustrated in Figure 13.

A control box containing only samples was used in this study. Control group, group I, II and III were buried in a different box. The moisture maintained as 20% - 40% by adding water with regular time intervals and it was measured by garden type moisture meter which is illustrated in Figure 14.

The specimens buried in soil were taken from the soil and washed gently with distilled water to remove the soil. The specimens recovered from soil were dried at 40^{o}C for 24 h in vacuum oven. Weight loss of the specimens with time was used to measure the degradation rate in the soil.

Before burial, 40 days after the burial and 76 days after the burial, the weights of the specimens were measured and recorded.

Figure 13: A photo from soil burial treatment

Figure 14: Moisture meter

CHAPTER 3

RESULTS AND DISCUSSION

3.1 FTIR Analysis

The chemical structures of the films were identified by ATR-FTIR spectroscopy. The FTIR spectra of LDPE and its blends with TPS are given in Figures 15 to 23.

In the spectrum of the LDPE film, peaks around 2918 and 2841 cm^{-1} correspond to $–CH_2$ asymmetric and symmetric stretching, respectively. The absorption band around 1464-1305 cm^{-1} can be assigned to the $–CH_2$ bending vibrations. . The strong peak at 712 cm^{-1} shows the $–CH_2$ rocking.

In the spectrum of thermoplastic starch, a broad peak in the range of 3593-3013 cm^{-1} corresponds to the –OH stretching and –CH stretching can be seen as a weak peak at 2942 and 2879 cm^{-1}. A broad band at around 1438-1330 cm^{-1} can be assigned to the –CH bending in the structure. The characteristic C-O stretching can be seen as a sharp peak at 1018 cm^{-1}.

In the spectrums of W20, W30 and W40, the peaks corresponding to LDPE and starch in the polymer structure are seen. The strong peaks at around 2918, 2847, 1457 and 718 cm^{-1} are related to the LDPE parts , the broad peak at 3370 cm^{-1} and the peak at 1030 cm^{-1} correspond to the starch units in the blend structure. Thus, incorporation of starch into the LDPE was achieved successfully.

The citric acid and stearic acid were added to the blend system to increase the compatibility between LDPE and TPS. Stearic acid has long alkyl groups and the carboxylic acid group in its structure. The citric acid characteristic –C=O peak at 1706 cm^{-1} and the stearic acid characteristic –C=O peak at 1707 cm^{-1} in the spectrums of the blends containing citric and stearic acid. The –OH stretching at around 3000 cm^{-1} related to the starch units was not observed in the blends with these additives, because of the interaction between the –OH groups in starch and the carboxylic acid groups of stearic acid and citric acid.

Cobalt(II) acetylacetonate, iron(III) stearate and manganese(II) stearate, which accelerate the photo and thermo oxidation of the polymers, give a polymer more susceptible to biodegradation. The absorption at 1712 cm^{-1} in the blends containing cobalt (II) acetylacetonate is attributed to the stretching of the carbonyl (C=O) group in cobalt(II) acetylacetonate.

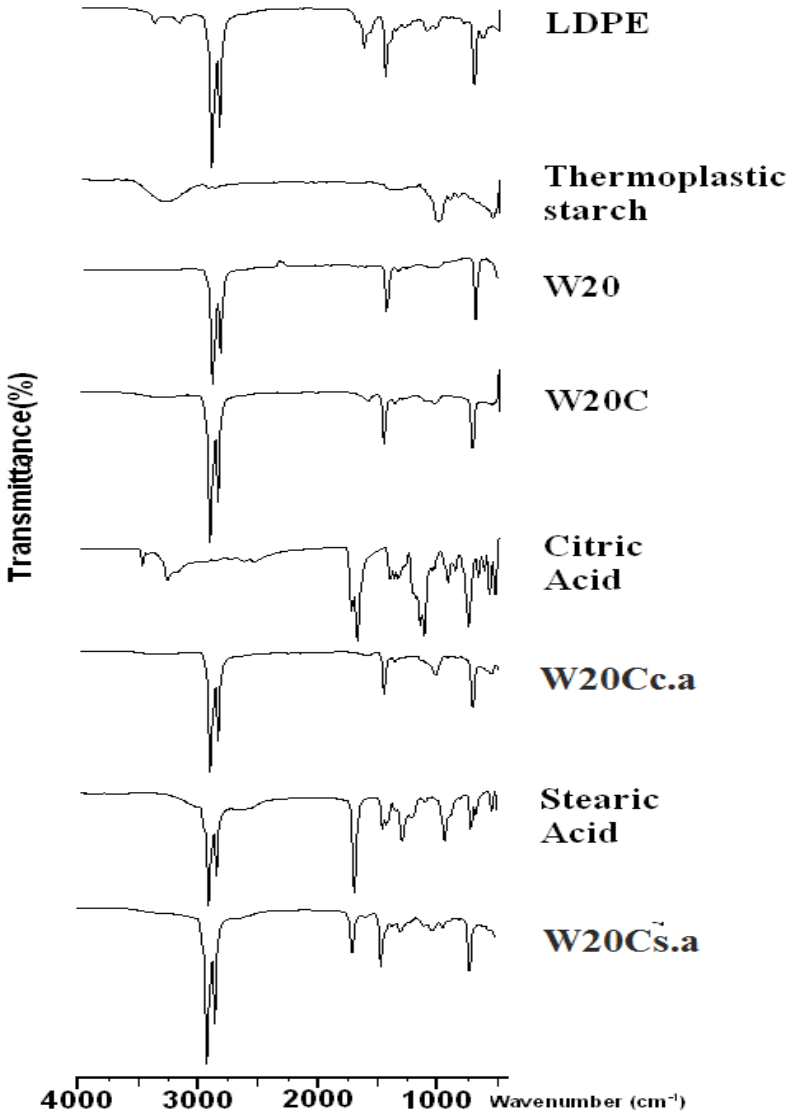

Figure 15: FTIR spectra of W20C,W20Cc.a and W20Cs.a from group I

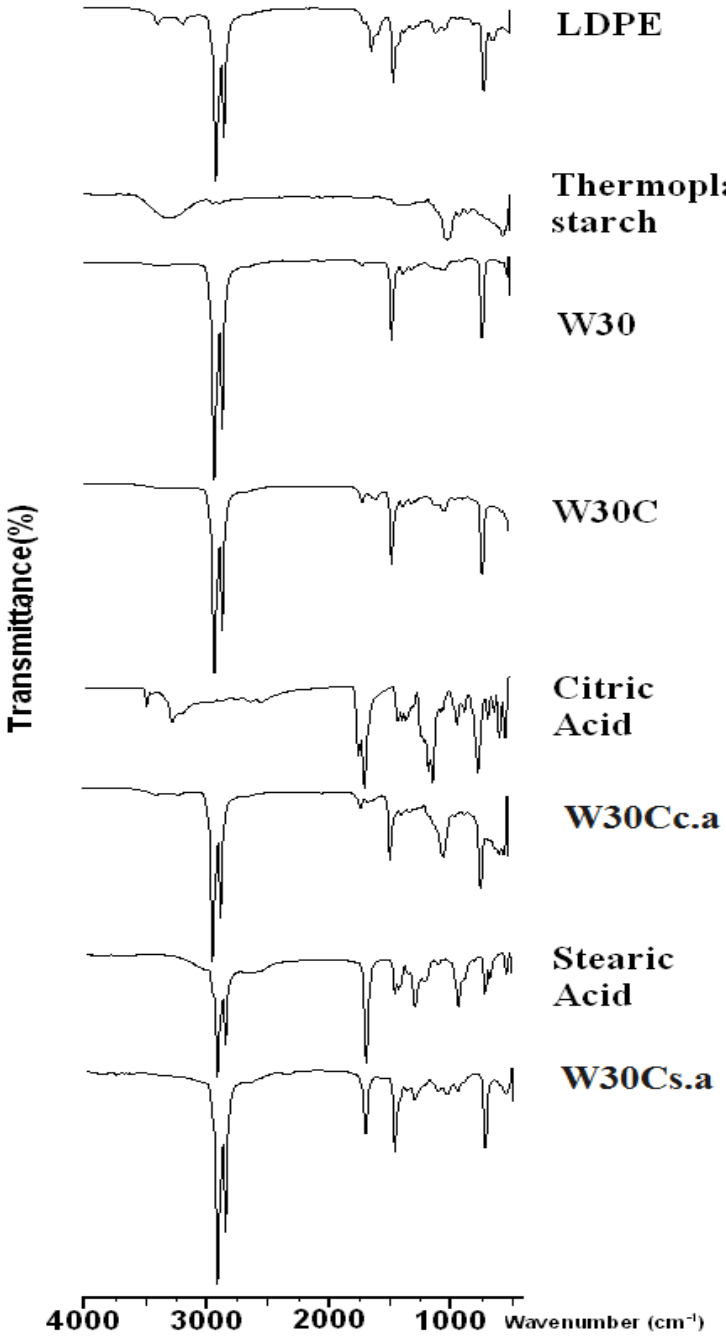

Figure 16: FTIR spectra of W30C, W30Cc.a and W30Cs.a from group I

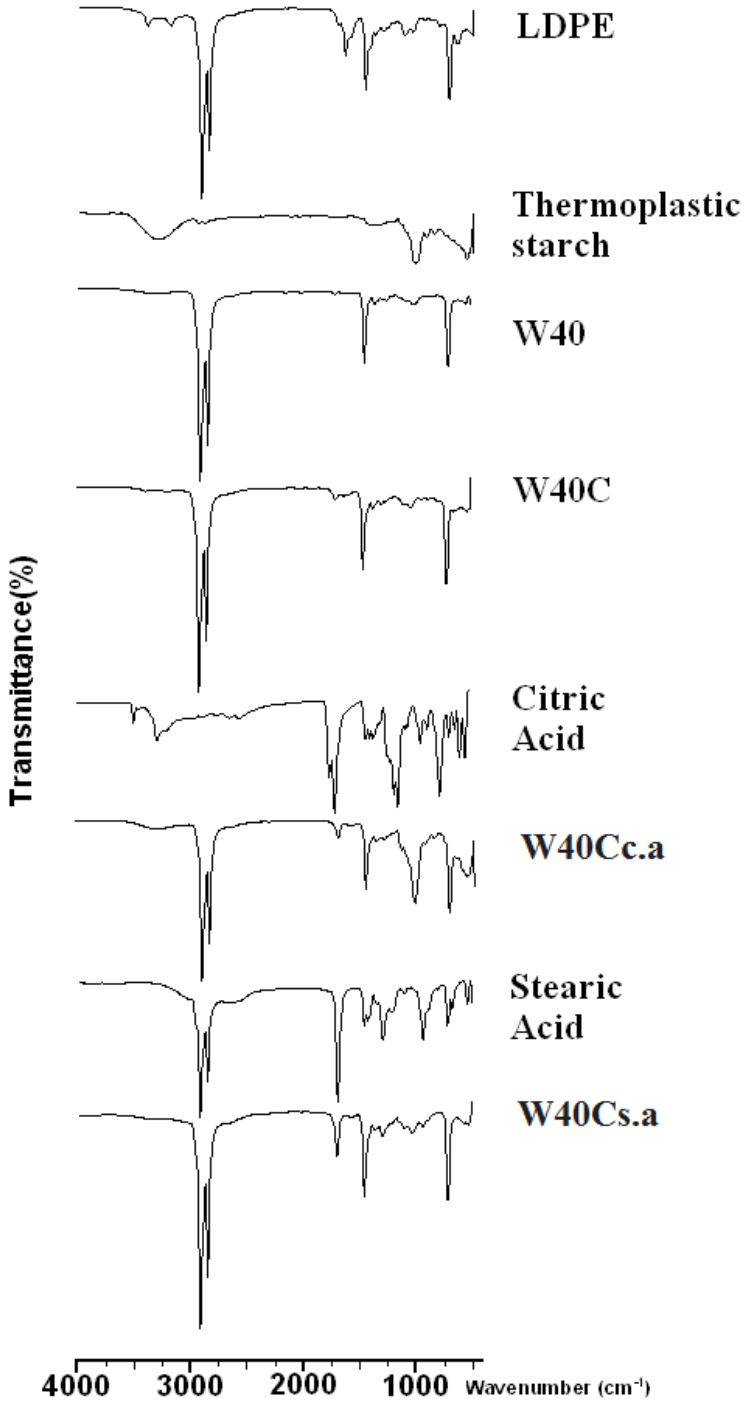

Figure 17: FTIR spectra of W40C, W40Cc.a and W40Cs.a from group I

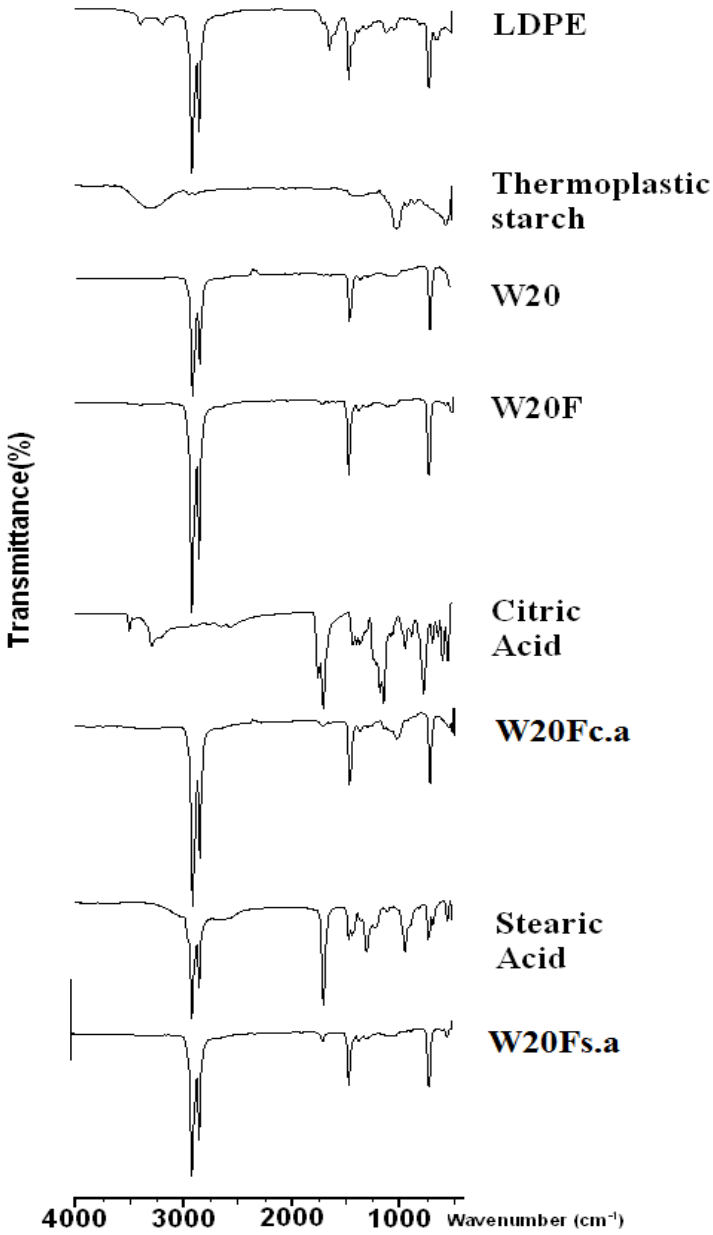

Figure 18: FTIR spectra of W20F, W20Fc.a and W20Fs.a from group II

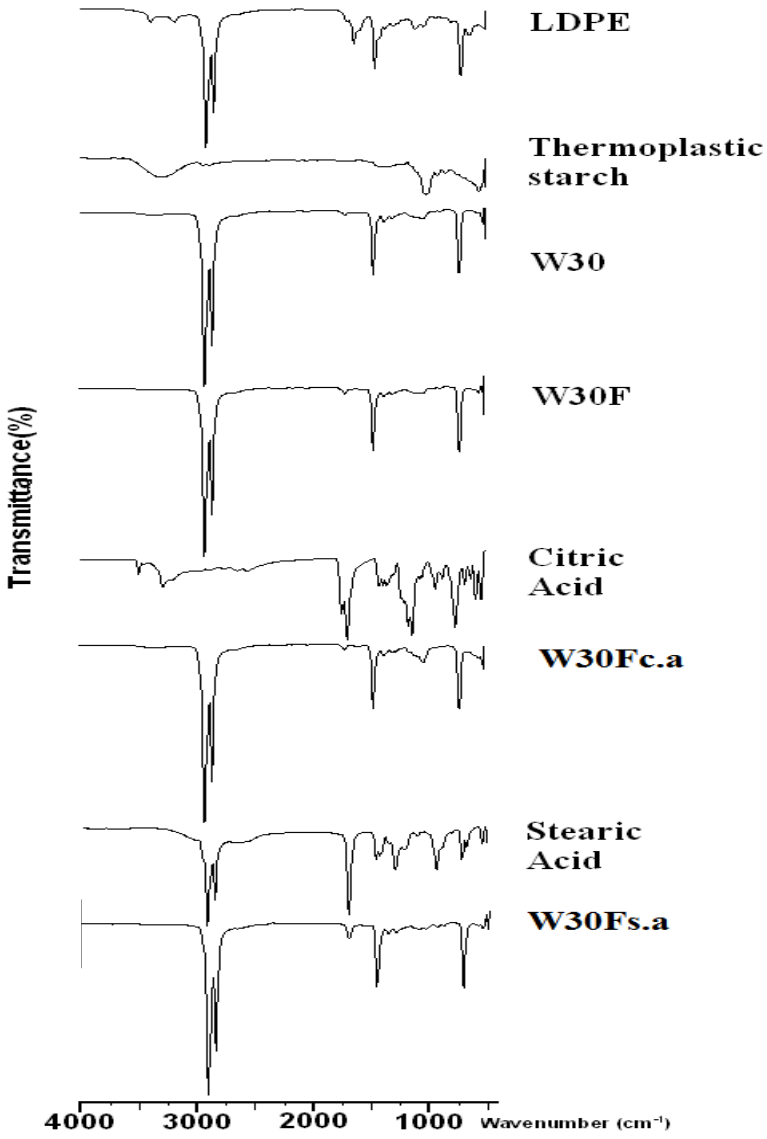

Figure 19: FTIR spectra of W30F, W30Fc.a and W30Fs.a from group II

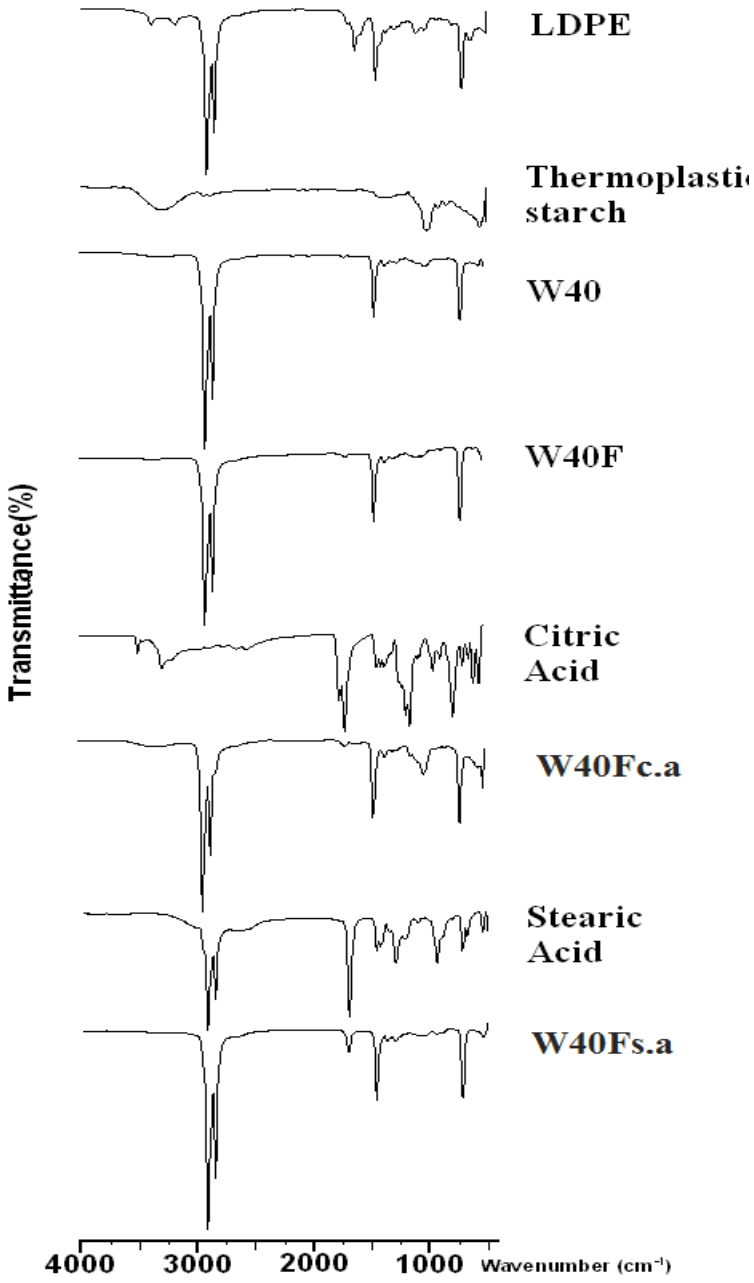

Figure 20: FTIR spectra of W40F, W40Fc.a and W40Fs.a from group II

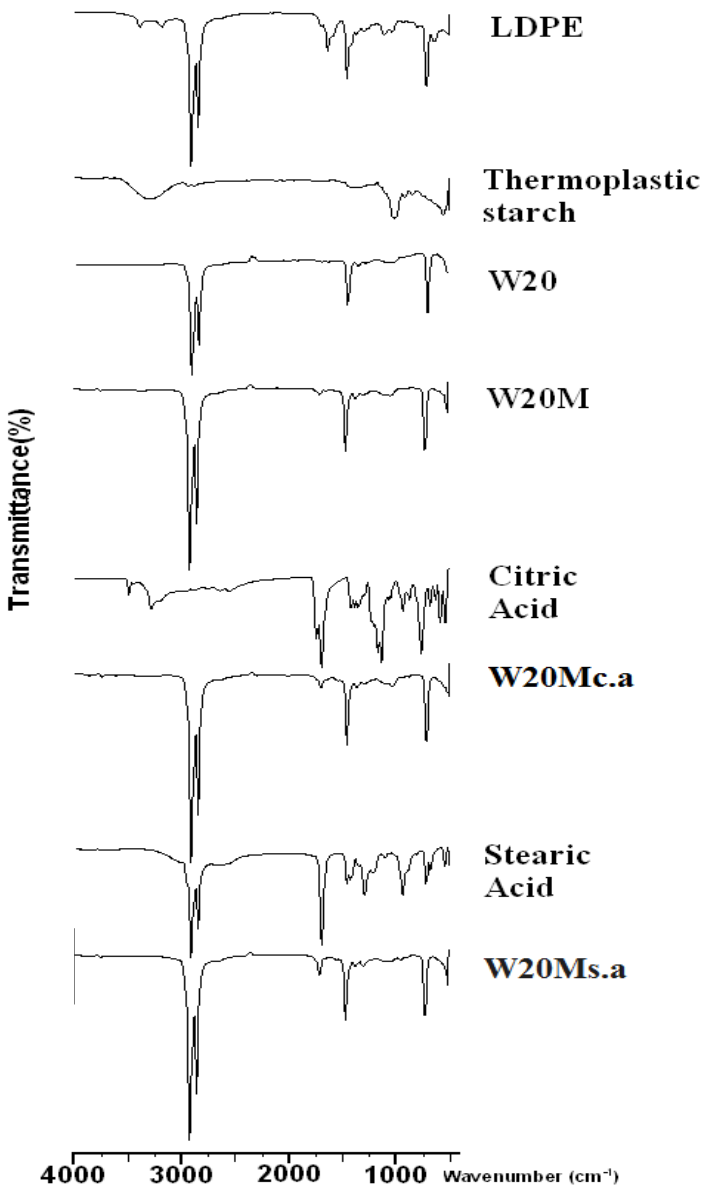

Figure 21: FTIR spectra of W20M, W20Mc.a and W20Ms.a from group III

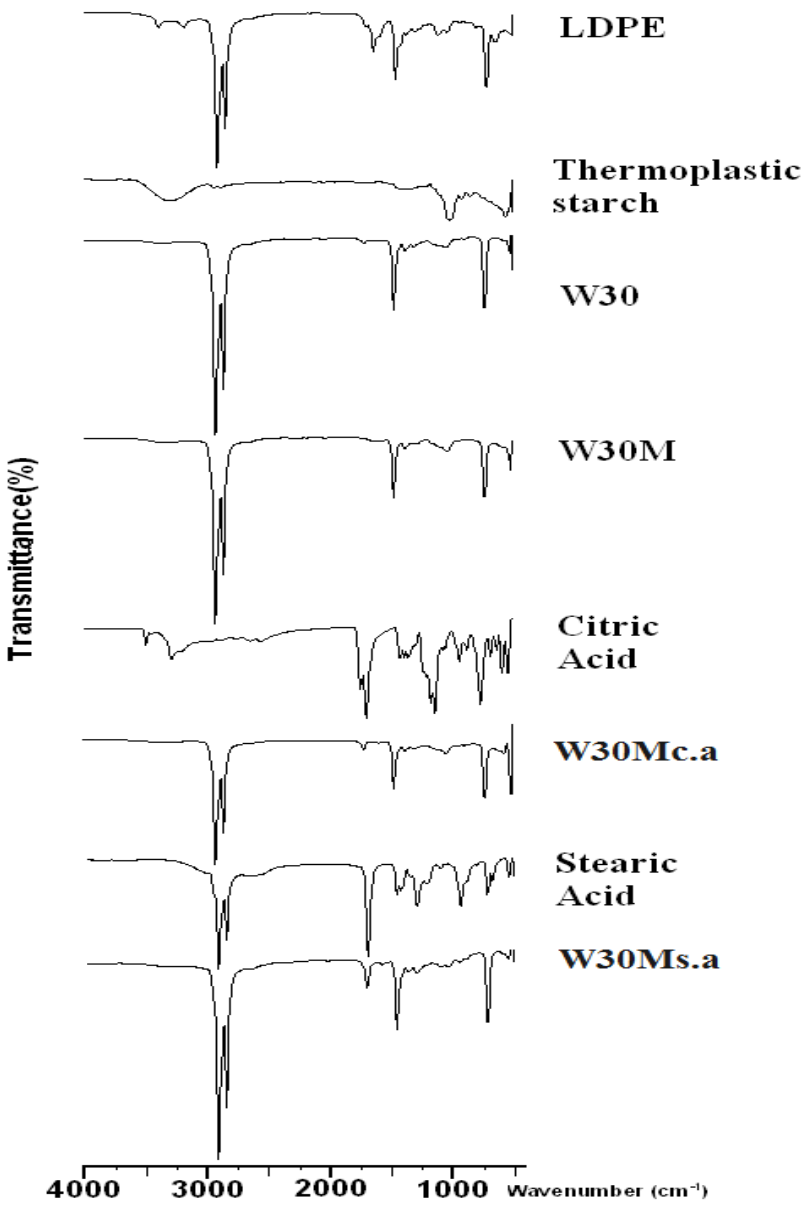

Figure 22: FTIR spectra of W30M, W30Mc.a and W30Ms.a from group III

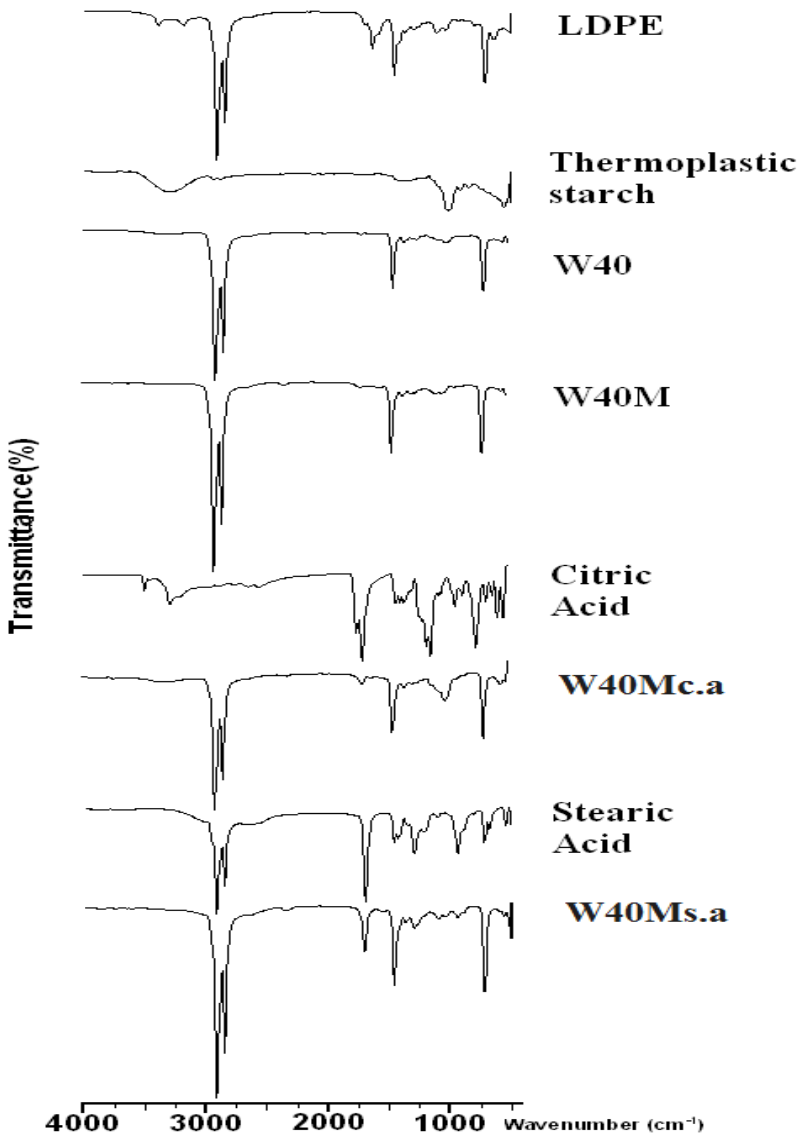

Figure 23: FTIR spectra of W40M, W40Mc.a and W40Ms.a from group III

3.2 Thermo Gravimetric Analysis

All the samples were analyzed by using thermo gravimetric analyser in order to observe their thermal stability.

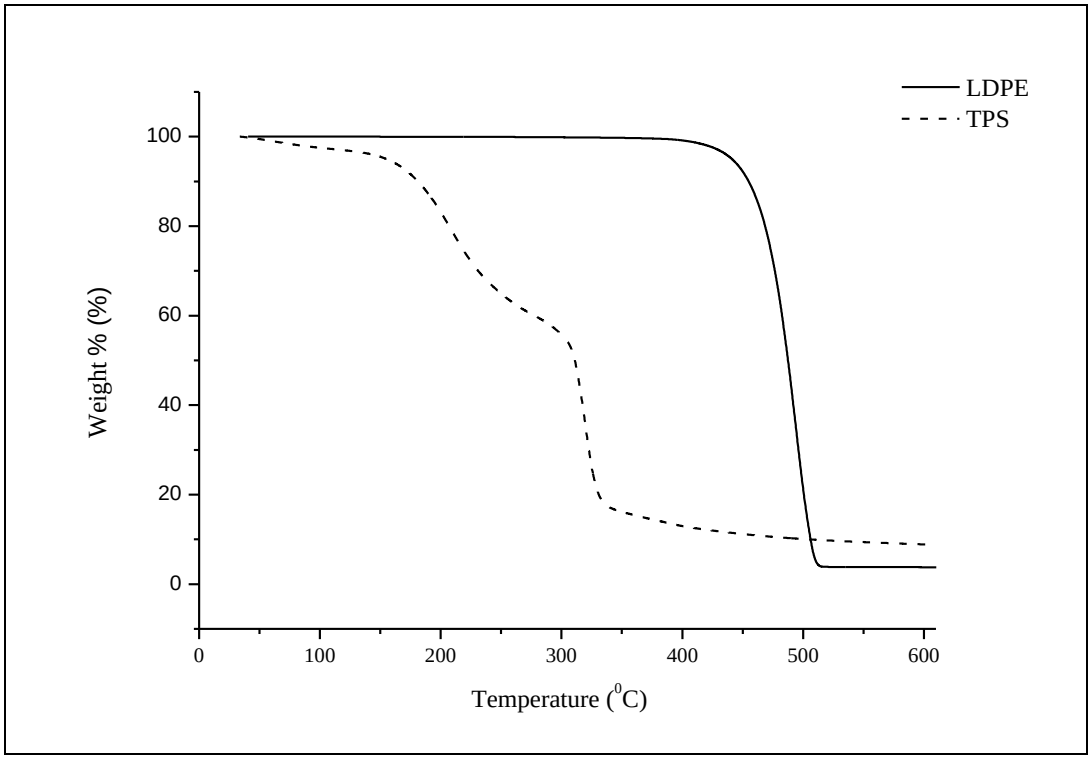

Figure 24: TGA curves of LDPE and TPS

The thermal degradation behaviour of LDPE and TPS are displayed in Figure 24. As The thermal decomposition of pure LDPE took place in a single stage, at 490 ^{0} C due to the fact that its carbonated chains decomposed during heating.

Thermoplastic starch showed three decomposition steps. The first step was observed around at 100^{0}C, which was attributed to the loss of moisture absorbed by the starch particles. The second degradation zone was observed around 210^{0}C, attributed to the

evaporation of glycerol. The last step was observed near 321^{0}C, in which decomposition of wheat starch was observed.

3.2.1 TGA Curves of Group I, Cobalt (II) acetylacetonate Group

TGA curves of group I are displayed in Figures 25, 26, 27 and the decomposition temperatures are given in Table 6. Four well defined weight loss stages can be observed in all the samples in the Group I. For all samples in group I, the first weight loss was attributed to the loss of moisture around 100^{0}C. The second weight loss was due to the evaporation of glycerol. The third mass loss is attributed to thermal degradation of the wheat starch and the last stage was attributed to the degradation of LDPE.

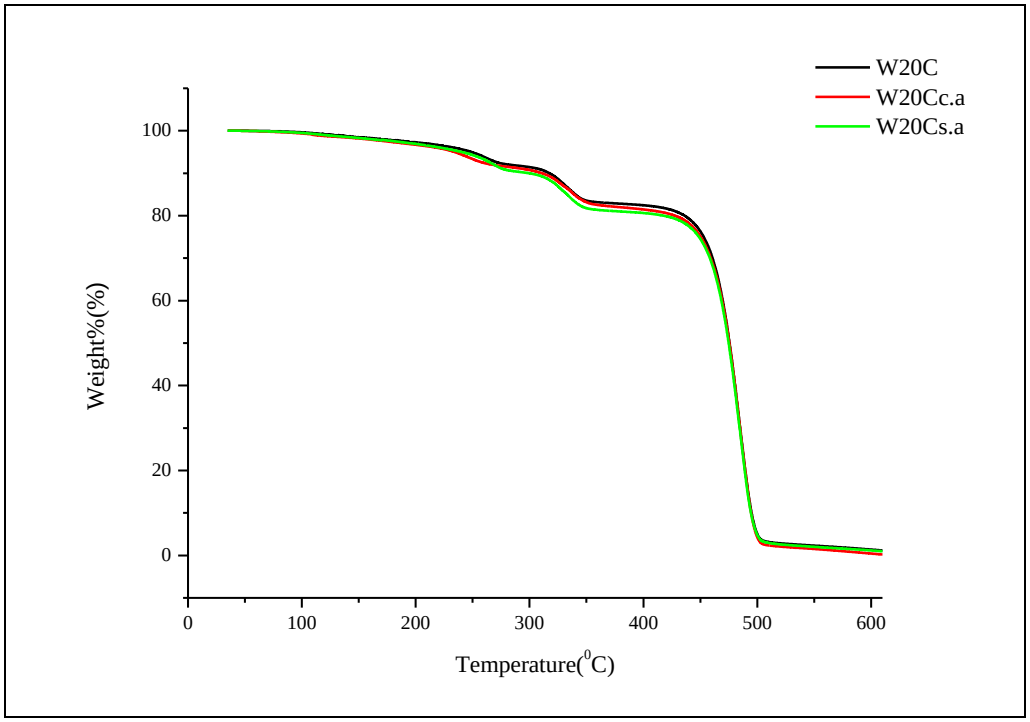

Figure 25: TGA curves of W20C, W20Cc.a and W20Cs.a from group I

TGA curves of the samples from group I, coded as W20C, W20Cc.a and W20Cs.a are displayed in Figure 25. The evaporation temperatures of the glycerol for the samples coded as W20C, W20Cc.a and W20Cs.a were 259^{0}C, 240 ^{0}C and 262^{0}C respectively. The degradation temperatures of the starch in films were 329^{0}C, 330 ^{0}C and 328^{0}C for W20C, W20Cc.a and W20Cs.a, respectively. The degradation temperature of LDPE for W20C, W20Cc.a and W20Cs.a was 482 ^{0}C, same for all.

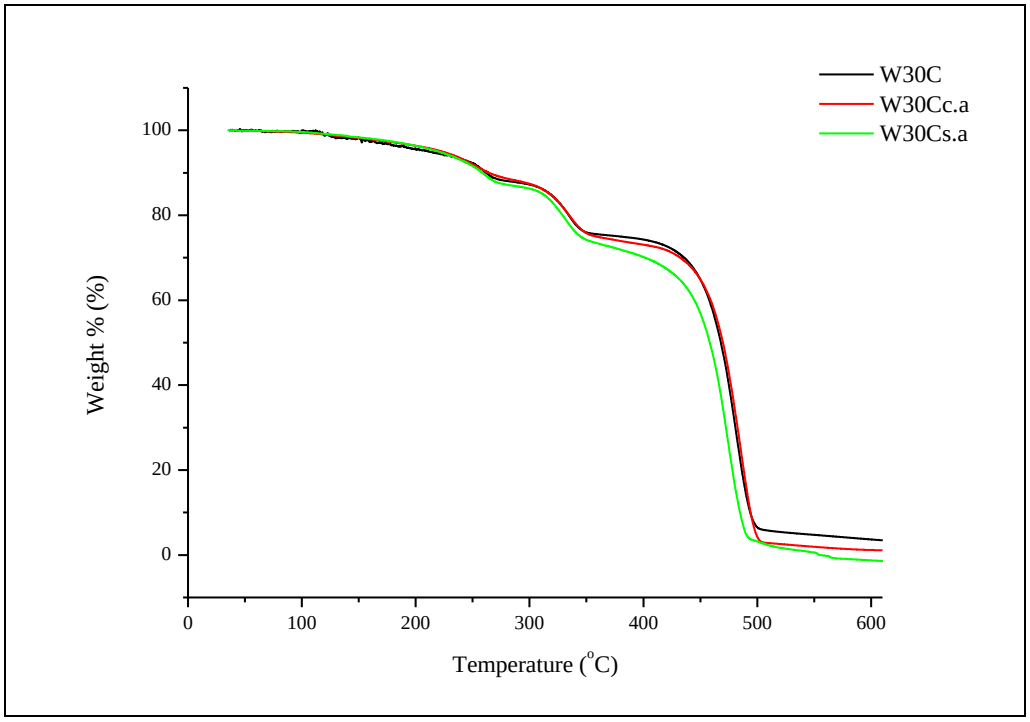

Figure 26: TGA curves of W30C, W30Cc.a, W30Cs.a from group I

TGA curves of the samples coded as W30C, W30Cc.a and W30Cs.a are displayed in Figure 26. The temperatures of evaporation of glycerol for W30C, W30Cc.a and W30Cs.a were 255^{0}C, 249 ^{0}C and 256^{0}C, respectively. The degradation temperatures of the starch in the blends were 329^{0}C, 331 ^{0}C and 326^{0}C for W30C, W30Cc.a and W30Cs.a, respectively. The degradation temperatures of LDPE were 477^{0}C, 482^{0}C and 471 ^{0}C for W30C, W30Cc.a and W30Cs.a, respectively.

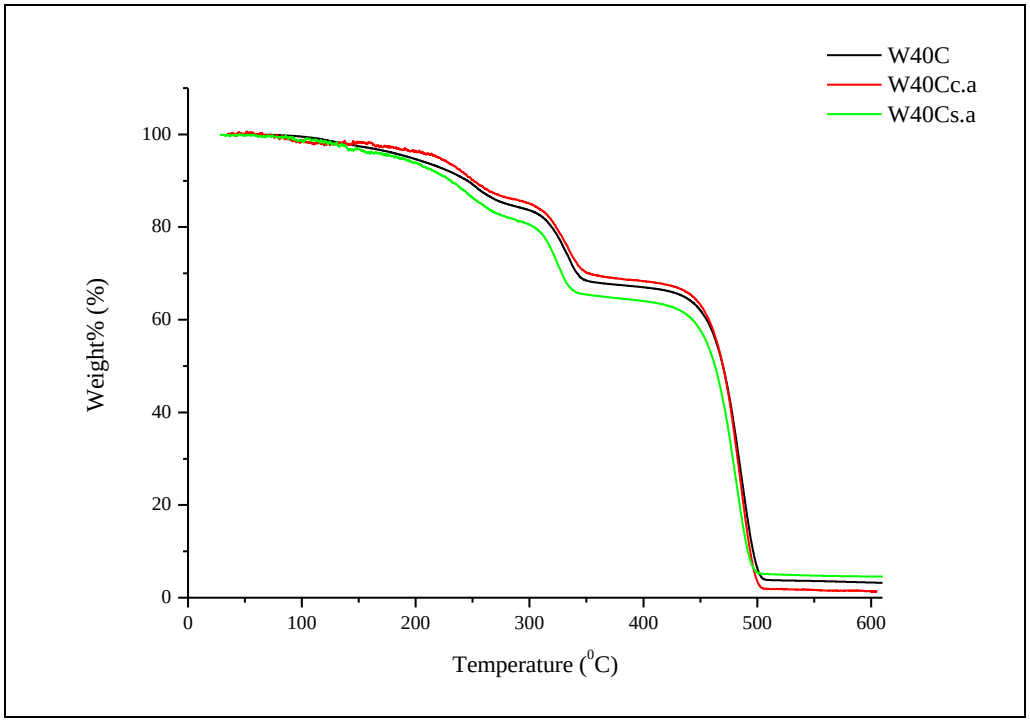

Figure 27: TGA curves of W40C, W40Cc.a, W40Cs.a from group I

TGA curves of the films which are coded as W40C, W40c.a and W40s.a are displayed in Figure 27. The temperatures of evaporation of glycerol for W40C, W40Cc.a and W40Cs.a were 249^{0}C, 240 ^{0}C and 254^{0}C respectively. The degradation temperatures of starch in the blends were observed at 328^{0}C, 332^{0}C and 323^{0}C for W40C, W40Cc.a and W40Cs.a, respectively. The degradation temperature of LDPE was 482^{0}C for W40C; it was 481^{0}C for W40Cc.a and W40Cs.a.

It is obvious that blending TPS with LDPE changed the decomposition temperature of starch and LDPE. The temperature of the decomposition of starch in neat TPS was 321^{0}C, but the decomposition temperatures of the starch in the films from group I were between 323 ^{0}C and 332 ^{0}C. The decomposition temperature of the neat LDPE was 490 ^{0}C where as this value varied from 477 to 482 ^{0}C for the blends in group I. Since glycerol was surrounded by LDPE, the evaporation temperature of glycerol increased dramatically.

Addition of citric acid with cobalt(II) acetylacetonate has decreased the evaporation temperature of glycerol since citric acid can form stronger hydrogen bonds with starch than glycerol. This effect was highly pronounced at the films with 40% of TPS loadings.

The addition of citric acid together with cobalt(II) acetylacetonate improved the thermal stability of starch in the blends. Also addition of citric acid lowered the evaporation temperature of glycerol, which indicates that citric acid can form stronger bonds than glycerol, resulting in lower temperatures of evaporation of glycerol.

Addition of stearic acid together with cobalt(II) acetylacetonate slightly increased the evaporation temperature of glycerol, which may indicate that the addition of stearic acid increased the interaction of glycerol with starch. Moreover, the addition of stearic acid together with cobalt(II) acetylacetonate, slightly decreased the thermal stability of starch through group I.

Table 6: The decomposition temperatures for group I before soil burial treatment

Code of the sample	Evaporation temperature of glycerol (^{0}C)	Decomposition temperature of starch (^{0}C)	Decomposition temperature of LDPE (^{0}C)
W20C	259	329	482
W20Cc.a	240	330	482
W20Cs.a	262	328	482
W30C	255	329	477
W30Cc.a	249	331	482
W30Cs.a	256	326	471
W40C	249	328	482
W40Cc.a	240	332	481
W40Cs.a	254	323	481

3.2.2 TGA Curves of Group II, Ferric Stearate Group

The TGA curves of group II are displayed Figures 28, 29, 30 and the decomposition temperatures of group II are displayed in Table 7.

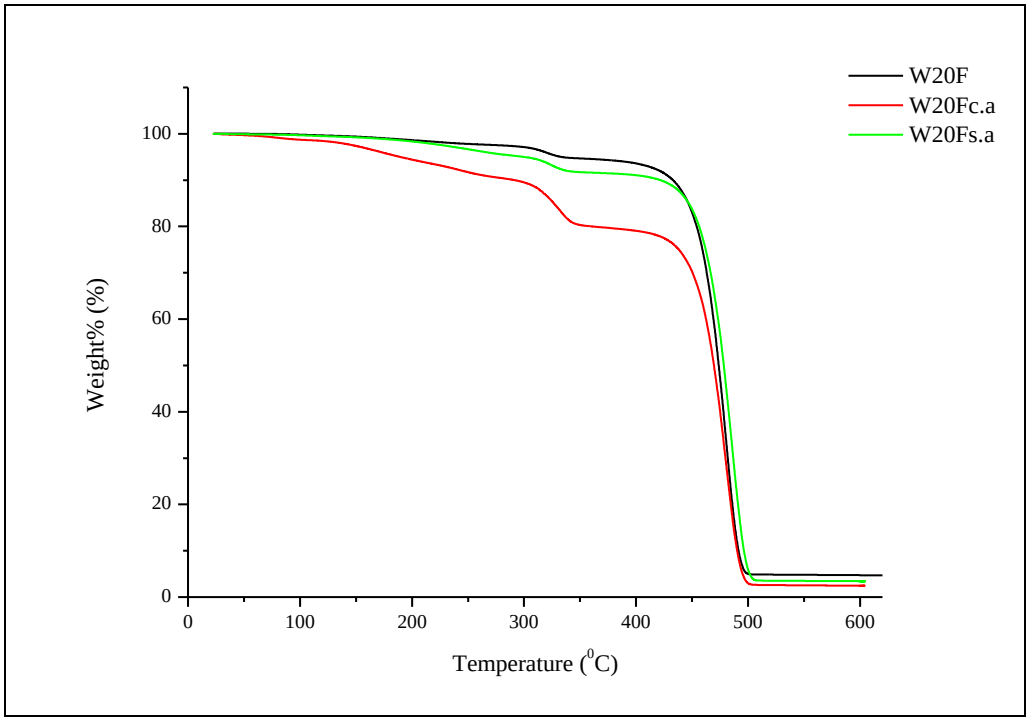

Figure 28: TGA curves of W20F, W20Fc.a and W20Fs.a from group II

Three well defined weight loss stages can be observed for 20% of TPS loadings. The first weight was attributed to the loss of moisture contents around 100^0C. The second weight loss was attributed to thermal degradation of the wheat starch. The last weight loss belongs to the degradation of LDPE. The mass loss which was attributed to evaporation of glycerol was not observed for the blends with 20% of TPS loadings. The degradation of starch was observed at 315 ^{0}C, 328^0C and 319^0C for the samples coded as W20F, W20Fc.a and W20Fs.a, respectively. The degradation temperature of LDPE was 478^0C for W20F, 479 ^{0}C for W20Fc.a and W20Fs.a.

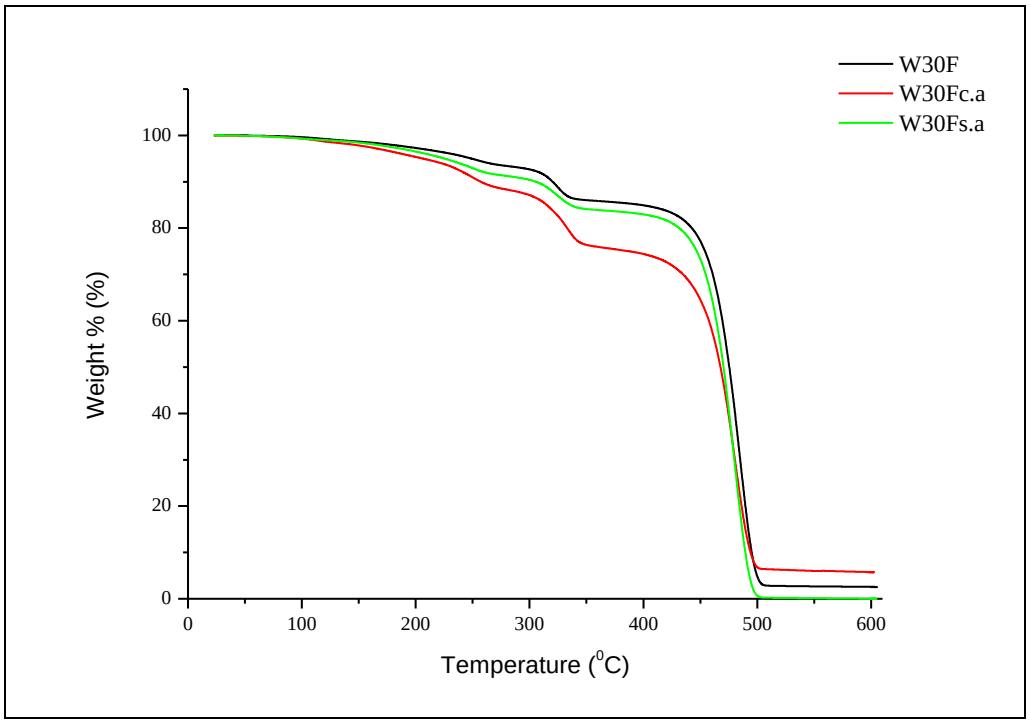

Figure 29: TGA curves of W30F, W30Fc.a, and W30Fs.a from group II

Four well defined weight loss stages were observed for 30% of TPS loadings. The first weight loss was attributed to the loss of moisture around 100^{0}C. The second weight loss was attributed to evaporation of glycerol. The third mass loss was attributed to thermal degradation of the wheat starch. The last weight loss stage belongs to the degradation of LDPE. The temperatures of evaporation of glycerol for W30F, W30Fc.a and W30Fs.a were 247^{0}C, 242^{0}C and 247^{0}C, respectively.

The degradation of starch was observed at 319 ^{0}C, 328^{0}C and 319^{0}C for W30F, W30Fc.a and W30Fs.a, respectively. The degradation temperatures of LDPE were 479^{0}C for W30F, 477^{0}C for both W30Fc.a and W30Fs.a.

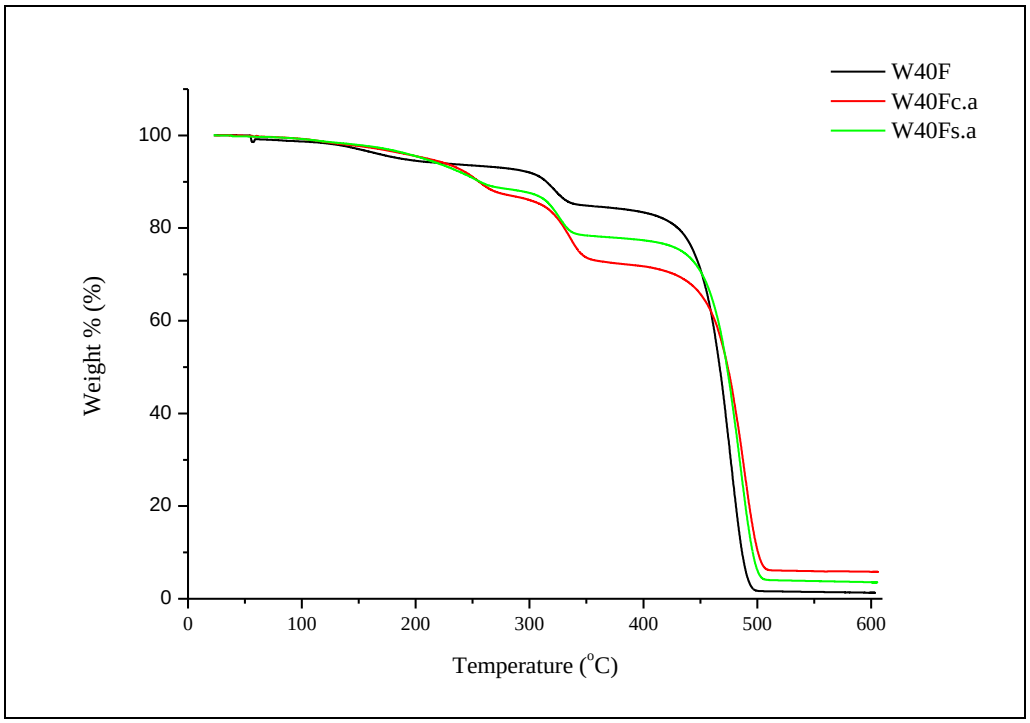

Figure 30: TGA curves of W40F, W40Fc.a and W40Fs.a from group II

The first weight loss was attributed to the loss of moisture around 100^0C for W40F, W40Fc.a and W40Fs.a. The weight loss attributed to evaporation of glycerol was not observed for W40F and the temperatures of evaporation of glycerol for W40Fc.a and W40Fs.a were 249^0C and 251^0C, respectively. The degradation of starch was observed at 317 ^{0}C, 330^0C and 321^0C for W40F, W40Fc.a and W40Fs.a. The degradation temperatures of LDPE were 475^0C, 481^0C and 481 ^{0}C for W40F, W40Fc.a and W40Fs.a.

It is obvious that blending TPS with LDPE changed the decomposition temperature of starch and LDPE. The temperature of the decomposition of starch in neat TPS was 321^0C, but the decomposition temperatures of the starch in the films from group II were between 315 ^{0}C and 330 ^{0}C. The decomposition temperature of the neat LDPE was 490 ^{0}C where as this value varied from 475 to 481 ^{0}C for the blends in group I. Since glycerol was surrounded by LDPE, the evaporation temperature of glycerol increased dramatically in some blends.

Through group II, it is obvious that addition of citric acid decreased the evaporation temperature of glycerol. Thermal stability of the starch was higher for the blends with citric acid, when they are compared to the rest of group II. Also, compared to the blends with just iron(III) stearate a slight increase in the thermal stability of starch was observed when iron(III) stearate was used together with stearic acid.

Table 7: The decomposition temperatures for group II before soil burial treatment

Code of the sample	Evaporation temperature of glycerol (^{0}C)	Decomposition temperature of starch (^{0}C)	Decomposition temperature of LDPE (^{0}C)
W20F	-	315	478
W20Fc.a	-	328	479
W20Fs.a	-	319	479
W30F	247	319	479
W30Fc.a	242	328	477
W30Fs.a	247	319	477
W40F	-	317	475
W40Fc.a	249	330	481
W40Fs.a	251	321	481

3.2.3 TGA curves of Group III, Manganese (II) Stearate Group

The TGA curves of group III are displayed in Figures 31, 32, 33 and tabulated in Table 8.

Four well defined mass loss stages can be observed in all the samples in group III. For all samples through the group the first weight loss was attributed to the loss of moisture contents around 100^0C.

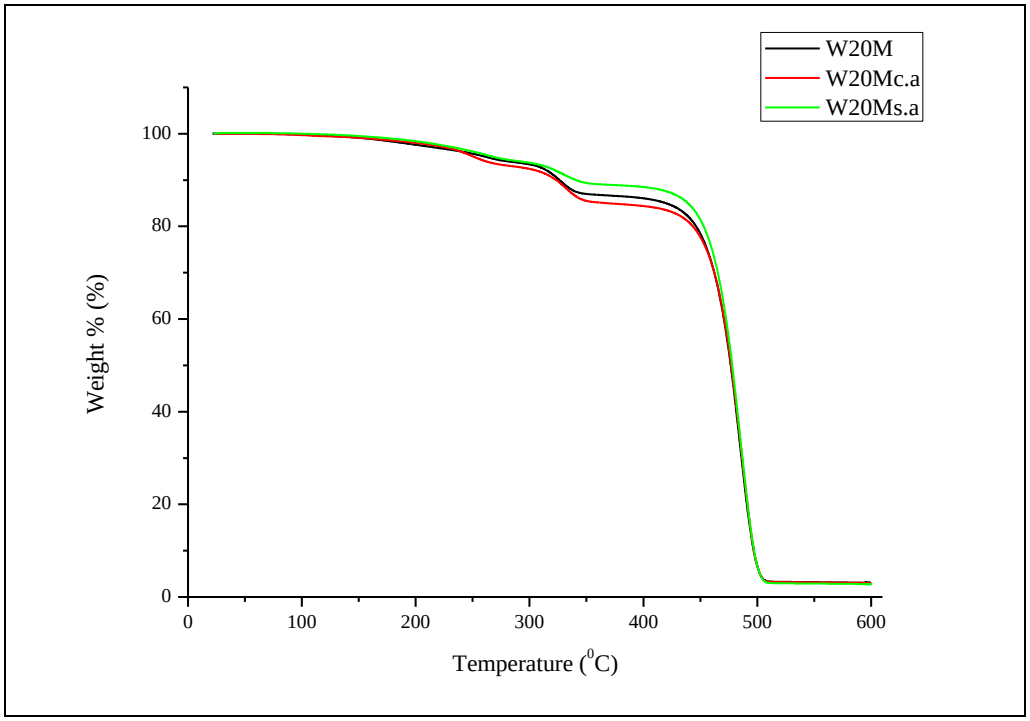

Figure 31: TGA curves of W20M, W20Mc.a and W20Ms.a from group III

TGA curves of the samples coded as W20M, W20Mc.a and W20Ms.a are displayed in Figure 31. The evaporation temperatures of glycerol for W20M, W20Mc.a and W20Ms.a were 259^{0}C, 245 ^{0}C and 261^{0}C respectively. The degradation temperatures of starch were observed at 322^{0}C, 326 ^{0}C and 324^{0}C for W20M, W20Mc.a and W20Ms.a. The degradation temperatures of LDPE for W20M, W20Mc.a and W20Ms.a were same for all, 481^{0}C.

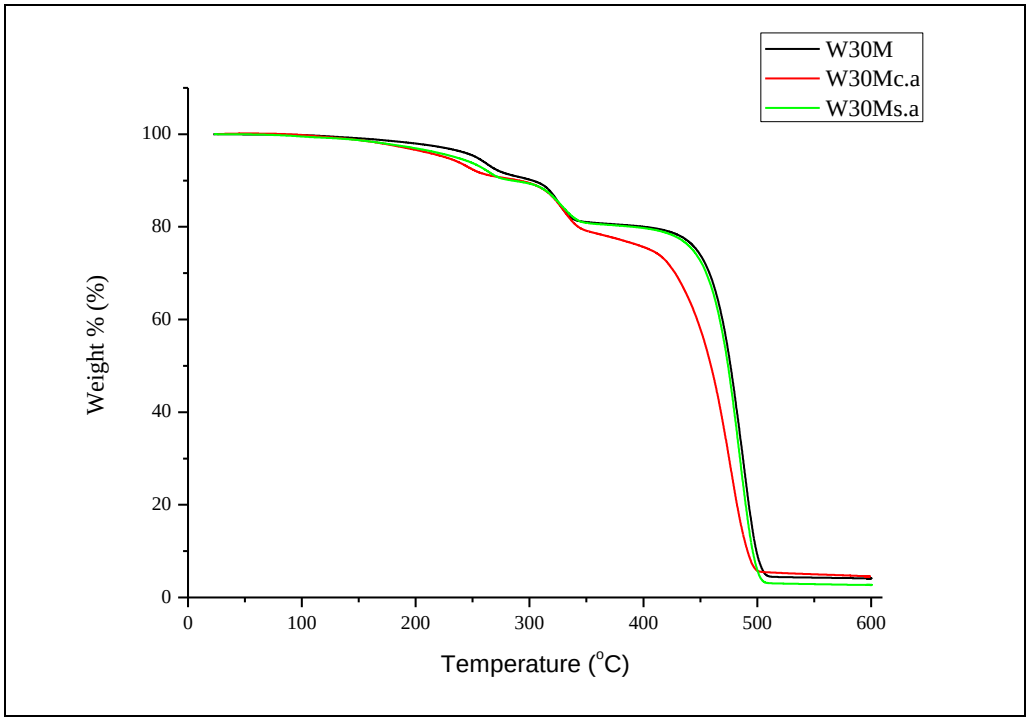

Figure 32: TGA curves of W30M, W30Mc.a and W30Ms.a from group III

TGA curves of samples coded as W30M, W30Mc.a and W30Ms.a are displayed in Figure 32. The temperatures of evaporation of glycerol for were W30M, W30Mc.a and W30Ms.a 258^{0}C, 241 ^{0}C and 258^{0}C respectively. The degradation of starch was observed at 321^{0}C, 326 ^{0}C and 325^{0}C for W30M, W30Mc.a and W30Ms.a. The degradation temperatures of LDPE for W30M, W30Mc.a and W30Ms.a were 481^{0}C, 473 ^{0}C and 481^{0}C, respectively.

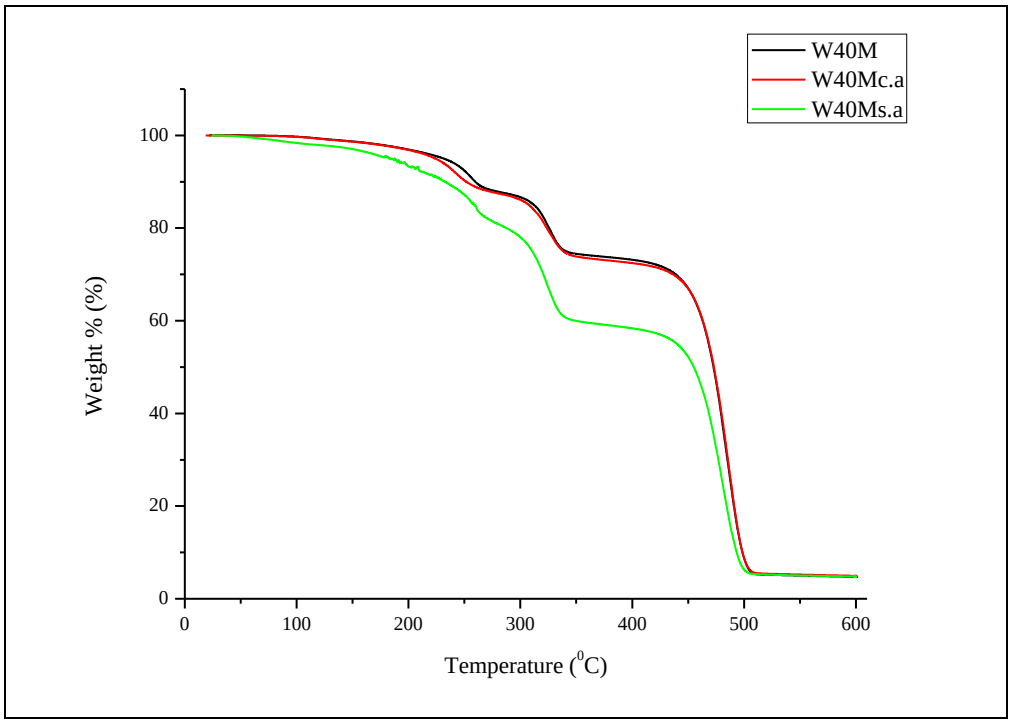

Figure 33: TGA curves of W40M, W40Mc.a and W40Ms.a from group III

TGA curves of the samples coded as W40M, W40Mc.a and W40Ms.a are displayed in the Figure 33. The evaporation temperatures of glycerol for W40M, W40Mc.a and W40Ms.a were 251^0C, 238^0C and 254^0C, respectively. The degradation of starch was observed at321^0C for W40M, W40Mc.a and W40Ms.a. The degradation temperatures of LDPE were same for W40M, W40Mc.a 481^0C, and 477^0C for W40Ms.a.

The addition of citric acid with manganese(II) stearate decreased the evaporation temperature of glycerol , resulted in a little improvement on the thermal stability of the starch in the blends. The same effect could be pronounced for the addition of stearic acid, the blends containing stearic acid the thermal stability of the starch slightly increased.

Table 8: The decomposition temperatures for group III before soil burial treatment

Code of the sample	Evaporation temperature of glycerol (^{0}C)	Decomposition temperature of starch (^{0}C)	Decomposition temperature of LDPE (^{0}C)
W20M	259	322	481
W20Mc.a	246	326	481
W20Ms.a	261	324	481
W30M	258	321	481
W30Mc.a	241	326	473
W30Ms.a	258	325	481
W40M	251	321	481
W40Mc.a	238	321	481
W40Ms.a	254	321	477

3.2.4 Comparison of TGA results of Group I, II and III

When the thermal stabilities of the starch in the blends are compared, it is obvious that pro–oxidants play a important role in this case. It is obvious that the highest thermal stability of the starch was observed in the group I among all three groups, in which cobalt(II) acetylacetonate used as pro-oxidant. This may indicate that this pro-oxidant acted as plasticizer and improve the stability of the starch.

Addition of iron(III) stearate significantly decreased the thermal stability of the starch in the blends. Only when it is used together with citric acid, a significant increase in the thermal stability of the starch was observed.

Addition of manganese (II) stearate had a moderate effect on the thermal stability of starch in the blends. When stearic acid is used together with this pro-oxidant a slight increase in the thermal stability of the starch in the blends. This effect was a result of high similarity between the structures of stearic acid and manganese(II) stearate.

Addition of citric acid decreased the evaporation temperature of glycerol in all groups. But when it is used with cobalt(II) acetylacetonate, it resulted in the lowest evaporation temperature of glycerol among all samples, in connection with it, the thermal stability of the starch was the highest among all samples. An explanation for this improvement is the combining effects of citric acid and cobalt(II) acetylacetonate. Also the similarity between their structures might have resulted in improvement on the thermal stability of starch.

All these shows that there is an interaction between the pro-oxidants and the compatabilizers despite the fact that amount of pro-oxidants are %0.5 by weight in all blends.

3.3. Mechanical Properties

The mechanical properties of the mulch films play an important role since they are exposed to stress during their lifetime. Tensile properties of control group, group I, II and III are given in Tables 9,10,11 and 12.

3.3.1 Mechanical Properties of Control Group

The tensile properties of the control group, which is prepared to see the effects of other additives on the mechanical properties and biodegradation rates are given in Table 9.

When TPS was introduced into the polymer matrix, a decrease in tensile properties was observed. At higher TPS contents, this effect was more pronounced. This trend was associated with the lack of compatibility between these two components, namely, TPS and LDPE.

The tensile strength of the films containing 20% TPS was 57.4% of the pure LDPE film. For higher TPS loadings, 30% and 40%, these values were 32.8% and 28.1% of the LDPE films respectively.

At higher loadings of TPS, starch granules have tendency to form aggregates. Because of the poor adhesion between TPS and LDPE, plus no compatibilizer was present in the blends; the transfer of stress through the blend was not efficient. Moreover, the tensile strength of the starch is lower than the tensile strength of LDPE [30]. All these factors resulted in decrease in tensile strength as the TPS content increased.

Since physical incorporation of starch in the matrix of LDPE that weakens the london forces between LDPE layers and the fact that TPS (starch is a low molecular weight polymer) has lower elongation compared to LDPE, reduction at elongation break was observed [36]. As recorded in Table 5, the percentage elongation at break value of the film containing 20% TPS, which is coded as W20, was 176.4 % where as this value for neat LDPE was 475,4%. When the TPS loadings reach to 30% and 40%, a dramatic change was observed, these values were 25,2 % and 18,4 % for W30 and W40, respectively.

Table 9: Mechanical properties of control group

Code of the sample	Ultimate tensile strength (MPa)	Elongation at break (%)
LDPE	14.8	475.4
W20	8.5	176.4
W30	4.9	25.2
W40	4.2	18.4

3.3.2 Mechanical Properties of Group I

Group I, in which cobalt (II) acetylacetonate was present as pro-oxidant, was tabulated in Table 10 in terms of its mechanical properties.

The general increase in the tensile strength and elongation at break values compared the samples in conrol group, is an evidence of Cobalt(II) acetylacetonate also act as a compatibilizer. Through group I, the addition of citric acid and stearic acid decreased the tensile strength of the films. This may be related to the acidity of stearic acid and citric acid, which caused the fragmentation and dissolution of the starch granules, causing the rigid structure of starch and resulting in diminished tensile properties

.

The elongation at break increases with the introduction of stearic acid and citric acid in to the blend. It indicates that citric and stearic acid increased the interfacial adhesion between LDPE and TPS. The samples with citric acid exhibited higher elongation at break values compared to films with stearic acid . Even at high loadings of TPS, for W40Cc.a 113,7 % elongation at break was observed, where as this value was 57,3 % for W40Cs.a. The elongation at break for W40 which does not contain any pro-oxidant and compatibizer was 18,4 % . The effect of citric acid when it is used with cobalt(II) acetylacetonate was seen more dramatically at high loadings of TPS.

Table 10: Mechanical properties of group I

Code of the sample	Ultimate tensile strength (MPa)	Elongation at break (%)
W20C	9.1	235.9
W20Cc.a	8.4	303.7
W20Cs.a	7.9	295.6
W30C	7.7	154.6
W30Cc.a	5.8	176.8
W20Cs.a	6.8	169.5
W40C	5.9	110.0
W40Cc.a	5.5	113.7
W40Cs.a	5.3	57.3

3.3.3 Mechanical Properties of Group II

Group II, in which iron(III) stearate was present as pro-oxidant, was tabulated in Table 11 in terms of its mechanical properties.

Addition of iron(III) stearate did not improved the mechanical properties of the blends. It is obvious that addition of stearic acid and citric acid decreased the tensile strength of the blends related to acidity of these additives.

Addition of stearic acid with iron(III) stearate decreased the elongation at break values in general through the group except at 40% of TPS loading. The percentage elongation at break value for W20Fs.a was 114.0 % which was lower than W20 (176.4%), W20F (183.2%) and W20Fc.a (262.9%). The similar trend was more dominant in the blends containig 30% of TPS. At higher loadings of TPS this trend was not observed. This may due to the fact that stearic acid may increase the distribution of TPS on LDPE, and this effect may more effective than the incompatibity between ferric stearate and stearic acid.

Addition of citric acid with Iron (II) stearate increased the elongation at break values all through the group. This sygnergetic effect is seen the at 20%, 30% and 40% TPS loadings. This effect was highly pronounced.at W30Fc.a. The Elongation at break value was 211.4% for W30Fc.a whereas this value for W30F was 27.4% and for W30Fs.a was 26.9%. W40Fc.a was the one having the highest elongation at break among the films with the films containing 40% of TPS.

Table 11: Mechanical properties of group II

Code of the sample	Ultimate tensile strength (MPa)	Elongation at break (%)
W20F	8.1	183.2
W20Fc.a	7.7	262.9
W20Fs.a	7.9	114.0
W30F	6.0	27.4
W30Fc.a	6.7	211.4
W30Fs.a	5.2	26.9
W40F	5.3	23.7
W40Fc.a	5.3	82.3
W40Fs.a	5.7	35.4

3.3.4 Mechanical Properties of Group III

Group III, in which manganese(II) stearate was present as pro-oxidant, was tabulated in Table 12 in terms of its mechanical properties.

.

Addition of manganese(II) stearate slightly improved the mechanical properties of the blends as it is tabulated in Table 12. It is obvious that addition of stearic acid and citric acid decreased the mechanical strength of the films.

Addition of citric acid with manganese(II) stearate decreased the elongation at break values in general through the group.

As tabulated in Table 12, addition of stearic acid with Manganase stearate slightly increased the elongation at break values except higher loadings of TPS, 40%.

Table 12: Mechanical properties of group III

Code of the sample	Ultimate tensile Strength (MPa)	Elongation at Break (%)
W20M	9.1	195.1
W20Mc.a	7.1	103.5
W20Ms.a	8.5	248.1
W30M	6.8	42.5
W30Mc.a	5.5	63.6
W30Ms.a	6.1	93.9
W40M	6.1	29.1
W40Mc.a	4.5	24.0
W40Ms.a	5.6	22.2

3.4 Soil Burial Treatment

The films had been buried under soil for 76. In order to investigate the degradation, weights of the films were measured with respect to time and the films recovered from soil were characterized by FTIR, subjected to mechanical testing and thermo gravimetric analysis were carried out.

3.4.1 Weight Loss

Soil has extensive microbial diversity, 1g of soil contains more than 10^7 prokaryotic cells and relatively, a large percent of them have not been identified. Microorganisms such as bacteria and fungi are involved in this process. Mainly, because of the low percolation rate, the soil burial method is known to be a slow process, but it reflects the real life conditions and gives key points about the biodegradation process taking place [37].

3.4.1.1 Weight Loss Records for Control Group

The percentage weight of the films from control group, namely for W20T, W30T and W40T with respect to time are displayed in the Figure 35. The graphs were plotted according to formula given in the Figure 34.

$$\textbf{Percentage Weight Loss} = \frac{(\text{Weight initial} - \text{Weight final})}{\text{Weight initial}} \text{x}100\%$$

Figure 34: The formula for the calculation for percentage weight loss

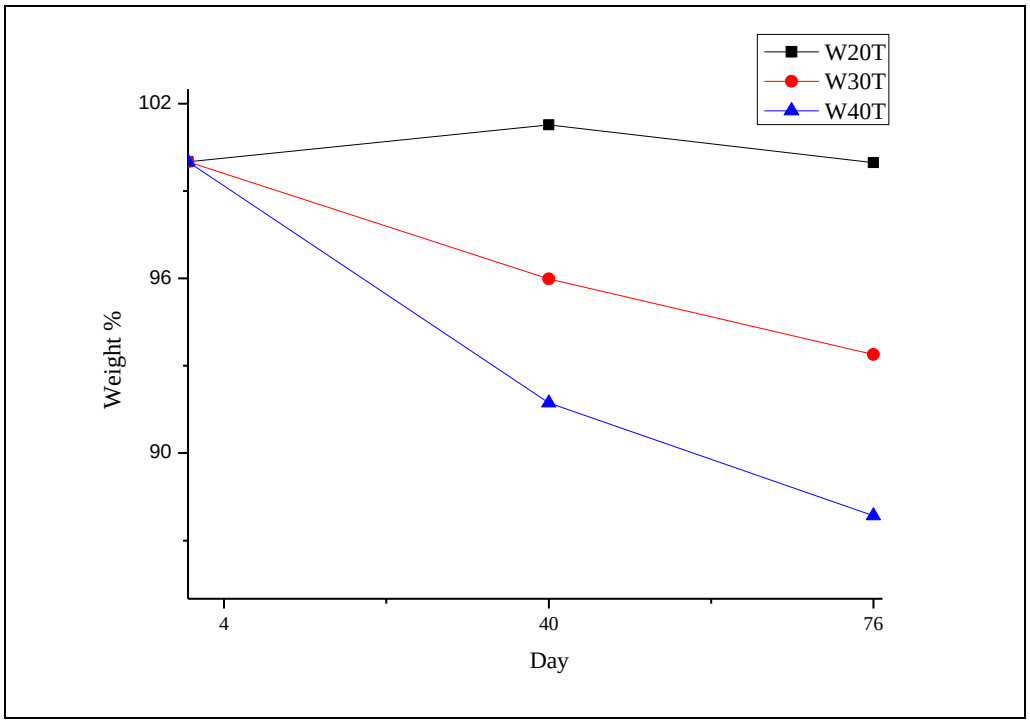

Figure 35: The percentage weight of the films from control group with respect to time

For W20, at the end of 40 days the sample did not lose weight, conversely, its weight increased by 1,72% of its initial weight. This increase may be a result of the hydrophilic character of TPS, which absorbs water in soil. At the end of 76 days, total weight loss for W20 was 0.27 % of its initial weight. For W30, the weight loss was recorded as 4.02% of its initial weight at the end of 76 days it lost its 6.61 % of its initial weight. For the sample coded as W40, the first weight loss was 8.29% of the initial weight and the total weight loss after 76 days was 12.15% of its initial weight. The entire amount of starch was not removed during the soil burial test. The explanation for this result is that TPS in some area of the blends were well protected by LDPE and not easily accessible to microbial action.

Increasing starch content in the blends speeded up the weight loss as it was expected and as mentioned in literature. Since dispersed parts of TPS started to join together become more interconnected and continuous, in blends containing higher percentage

of TPS, for the films with 30% and 40% TPS content, the weight loss became more significant. These results are in close agreement with the percolation analysis performed by Peanasky and Wool [37]. In order to explain the accessibility of starch in polyethylene/starch blends, Peanasky and Wool, used the percolation theory in mathematics, which analyzes the connectivity of one component in a randomly dispersed in another.

These authors claimed that the microbial attack started from the top and bottom of the polymer films by computer simulation. The percolation thresold is the minumum level of starch needed to connectivity between starch domains. The accessibility of starch is highly dependent on an apparent percolation threshold near 30% by volume or approximately 40% by weight of starch. Below the percolation thresold the consumption of starch by microorganisms is not efficient [37]. Thus for high TPS containing blends, a very small amount of TPS was protected by the LDPE, as a result higher degradation rates were observed.

3.4.1.2 Weight Loss Records for Group I

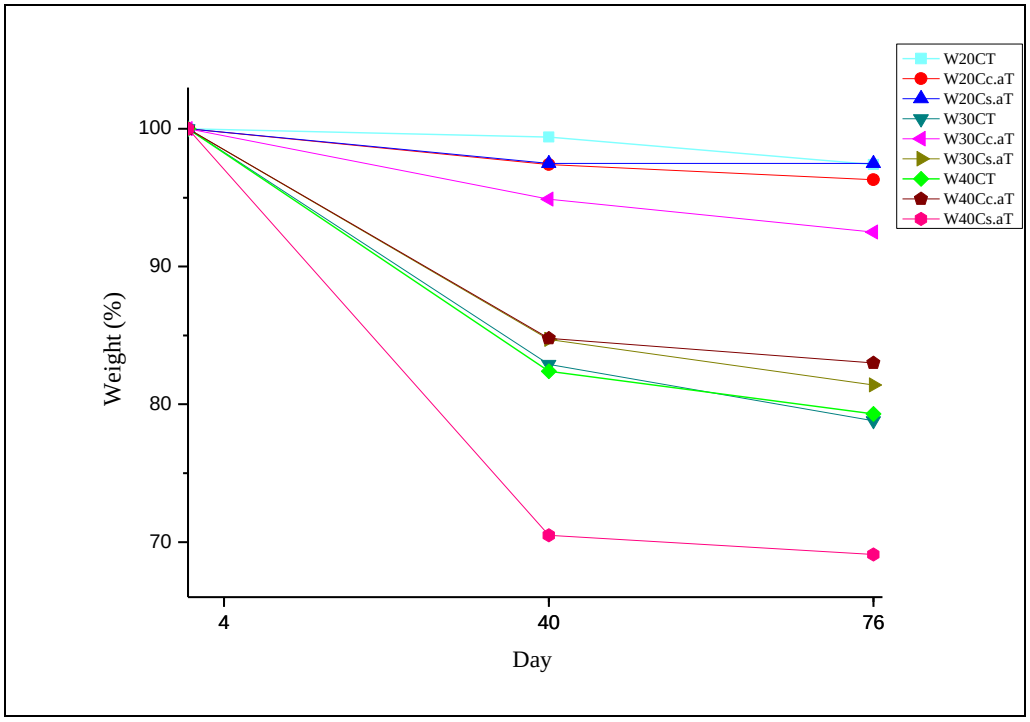

Figure 36: The percentage weight of the films from group I with respect to time

The percentage weights of the films are displayed in Figure 37. After 40 days of burial the weight loss for W20C, W20Cc.a and W20Cs.a were 0.63 %, 0.34 % and 1.77% of their initial weight, respectively. At the end of 76 days total weight loss for W20C, W20Cc.a and W20Cs.a were 2.62%, 3.75% and 2.47% of their initial weights, respectively.

At the end of 40 days, the weight loss for W30C, W30Cc.a and W30Cs.a were 17.14 %, 5.07% and 15.26% of their initial weights, respectively. At the end of 76 days total weight loss for W30C, W30Cc.a and W30Cs.a were 21.20 %, 7.53 % and 18.61 % of their initial weight, respectively.

For high loadings of starch, the weight loss for W40C, W40Cc.a and W40Cs.a were 17.14 %, 15.16 % and 29.55 % respectively after 40 days. At the end of 76 days

total weight loss for W40C, W40Cc.a and W40Cs.a were 20.73 %, 16.91 % and 30.99 % of their initial weight, respectively. Since degradation started by starch consumption, the weight loss was due to the fact that loss of glycerol, citric and starch. The weight loss data show that the films with citric acid content showed the least weight loss. Since starch and citric acid may form strong interactions in the presence of cobalt(II) acetylacetonate, causing stability and resulting low consumption of starch.

3.4.1.3 Weight Loss Records for Group II

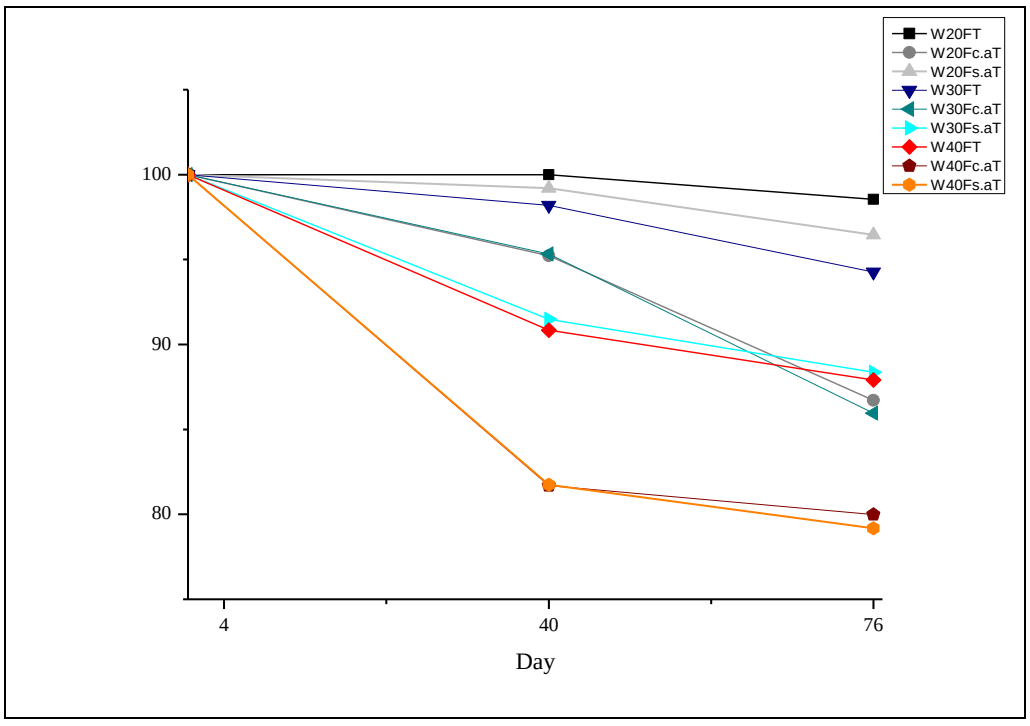

Figure 37: The percentage weight of the films from group II with respect to time

The percentage weights of the films are displayed in Figure 36. For loadings of 20 % of TPS, similar trend in control group was observed. The entire amount of starch content was not removed due to the high LDPE content. The weight of the sample

coded as W20F did almost not change during 40 days period. At the end of 76 days, the weight loss for W20F was 1.45% of its initial weight. W20FC.a lost 4.78 % of its initial weight after 40 days, at the end of 76 days it was 13.29 %. The weight loss for W20Fs.a was 0.87 % of its initial weight after 40 days and total weight loss was 3.59 % of the initial weight of the sample.

After 40 days of burial the weight loss for W30F, W30Fc.a and W30Fs.a were 1.81 %, 4.67% and 8.52%, of their initial weight respectively. At the end of 76 days total weight loss for W30F, W30Fc.a and W30Fs.a were 5.73%, 14.03 % and 11.65%, respectively.

For high loadings of starch, the weight loss for W40F, W40Fc.a and W40Fs.a were 9.16 %, 18.32 % and 18.27 % of their initial weights, respectively after 40 days. At the end of 76 days total weight loss for W40F, W40Fc.a and W40Fs.a were 12.09 %, 20.01 % and 20.82% of their initial weights, respectively.

Through group II, it is evident that increasing starch content increased the weight loss which agrees with the percolation theory. The blends containing high percentage of starch, 40%, degraded rapidly in the first 40 days, over the next 36 days a gradual decrease in degradation rate was observed. This rapid fall in weights of the blends were caused by the removal of low molecular weight substances such as glycerol and consumption of starch by microorganisms. The highest weight loss was observed in the blends with citric acid. This is an evidence that when citric acid used together with iron(III) stearate improved the dispersion of TPS in LDPE and created more possible substrates for the microorganisms. Another explanation for high amounts of degradation in the samples with citric acid that citric acid caused badly acidolyisis of starch, deteriorated the rigid structured of starch and eased the consumption by the micro-organisms.

3.4.1.4 Weight Loss Records for Group III

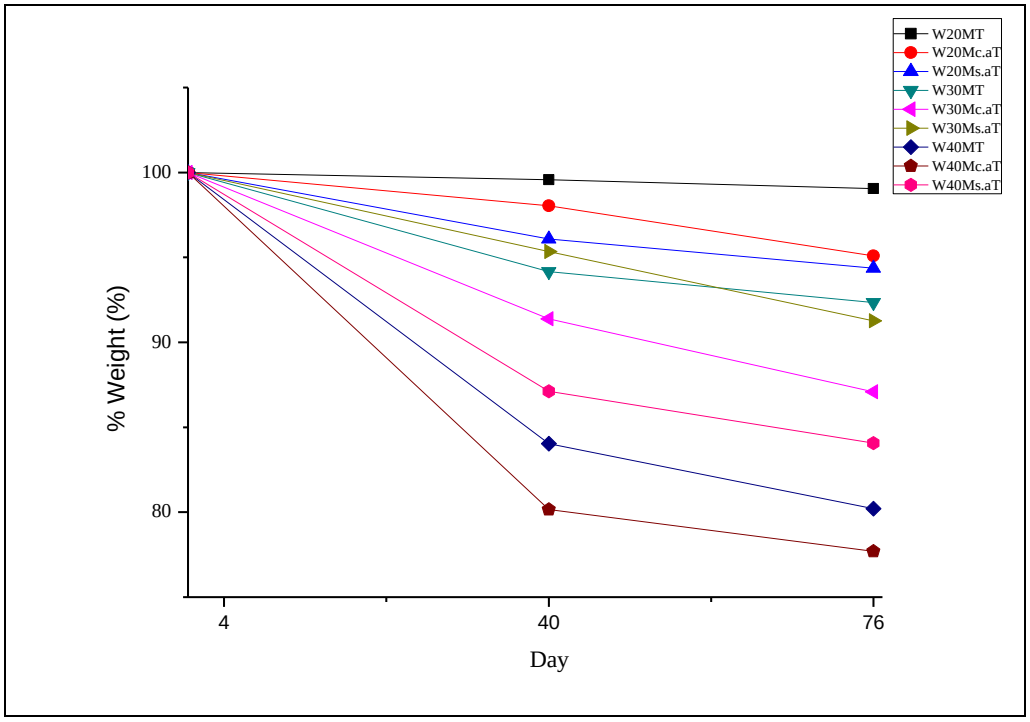

Figure 37: The percentage weight of the films from group III with respect to time

After 40 days of burial the weight loss for W20M, W20Mc.a and W20Ms.a were 0.42 %, 1.96 % and 3.92 % of their initial weight, respectively. At the end of 76 days total weight loss for W20M, W20Mc.a and W20Ms.a were 0.96 %, 4.91 % and 5.64 %, respectively.

At the end of 40 days of soil burial, the weight loss for W30M, W30Mc.a and W30Ms.a were 5.83%, 8.62% and 4.66 % of their initial weight, respectively. At the end of 76 days total weight loss for W30M, W30Mc.a and W30Ms.a were 7.62%, 12.91 % and 8.54 %, of their initial weight, respectively.

For high loadings of starch, the weight loss for W40M, W40Mc.a and W40Ms.a were 15.96 %, 19.84 % and 12.89 % respectively after 40 days. At the end of 76

days total weight loss for W40M, W40Mc.a and W40Ms.a were 19.79 %, 22.31 % and 15.94%, of their initial weight, respectively.

3.4.2. FTIR Analysis After Soil Burial Treatment

The FTIR spectra of the samples from control group, group I, II and III are displayed in Figures 38 to 47. The spectra of the films recovered from soil are notified with star.

A broad peak around 3500 cm^{-1} corresponding to –OH stretching was observed in the spectra of the films recovered from soil. That shows that degradation starts from starch, more –OH group became free. This trend is more dominant for films with 40% of starch and for the films with citric acid and stearic acid. Since, these additives interacted with the –OH group of starch, with removal of these additives by micro organisms, more –OH group became free, and stronger peakwas observed compared to before soil burial.

The citric acid and stearic acid characteristics -C=O peaks around 1700 cm^{-1} were not observed in the structure of the films with stearic and citric acid after soil burial. This indicates that during soil burial these additives were removed by micro-organisms.

FTIR spectra of the samples recovered from soil show that a broad peak around 1640 cm^{-1} assigned to -OH band was observed since the films under soil absorbed water.

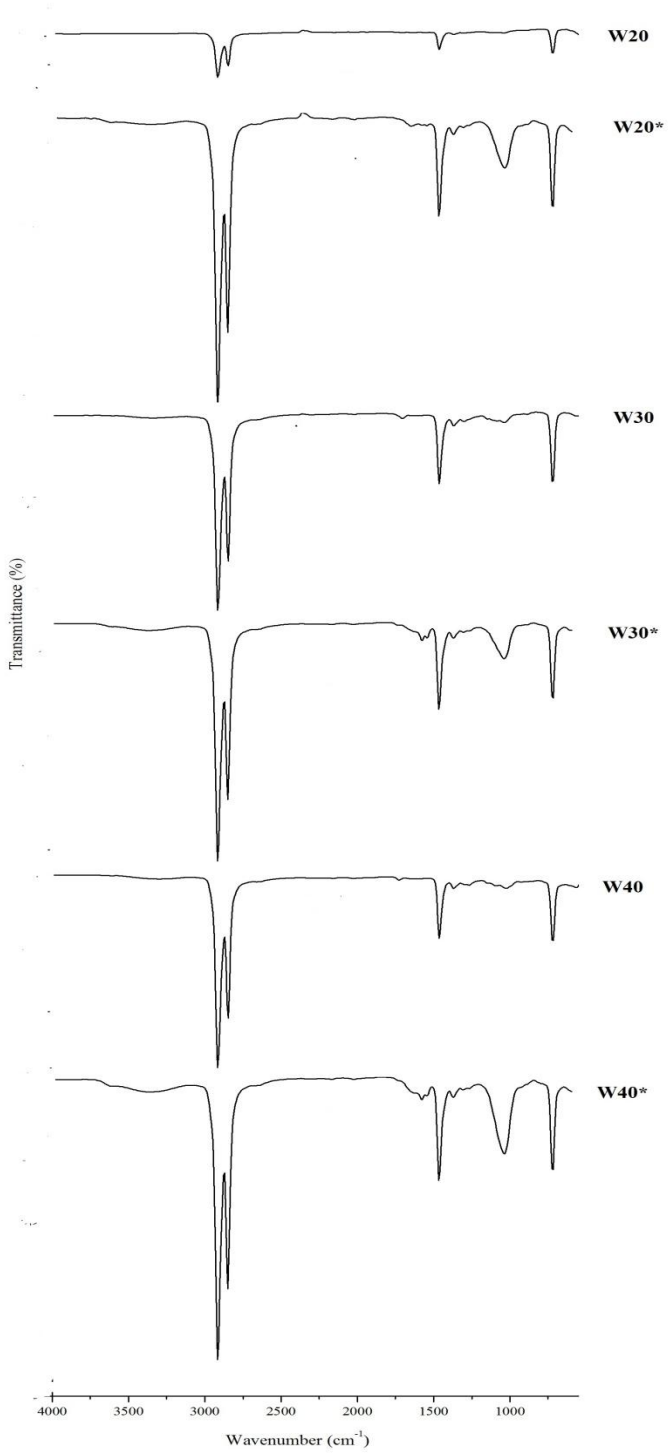

Figure 38: FTIR spectra of control group before and after soil burial treatment

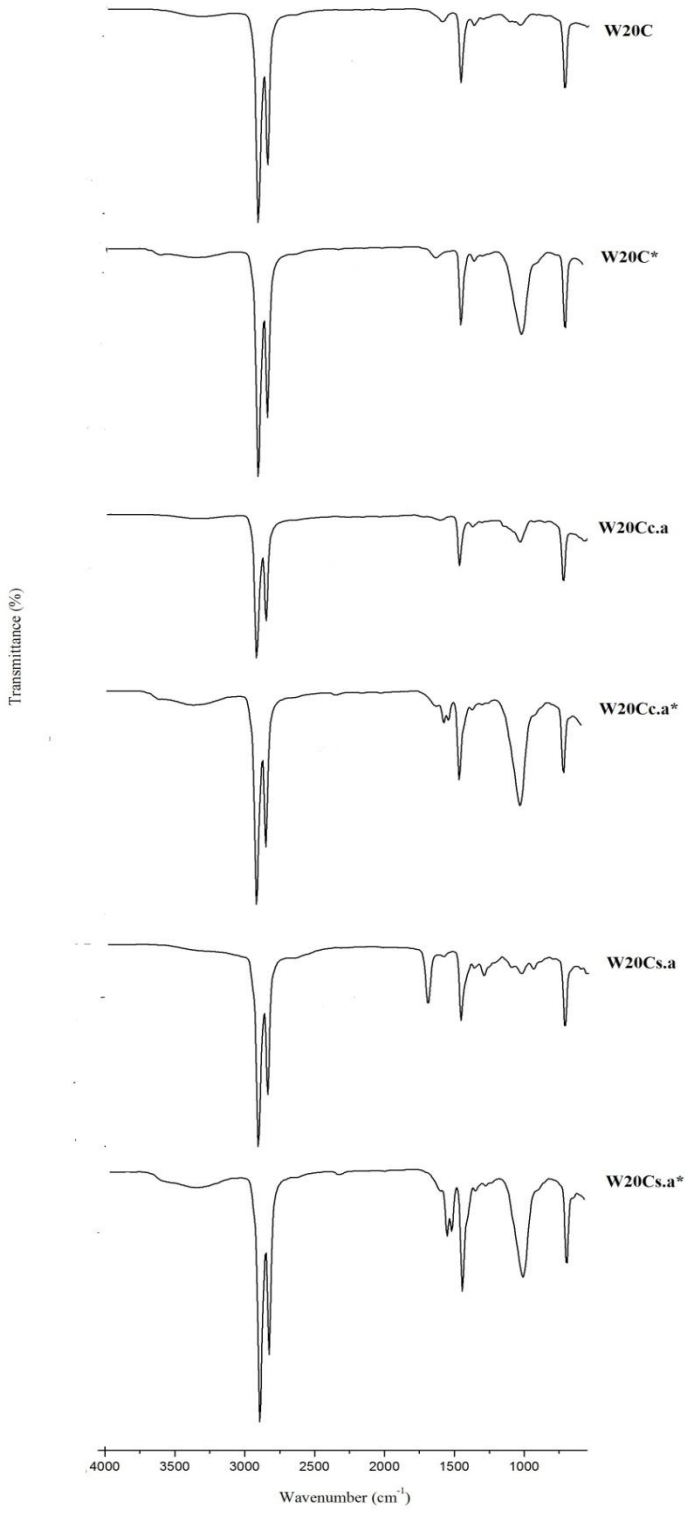

Figure 39: FTIR spectra of the films with 20% TPS loadings from group I before and after soil burial treatment, soil burial notified with star

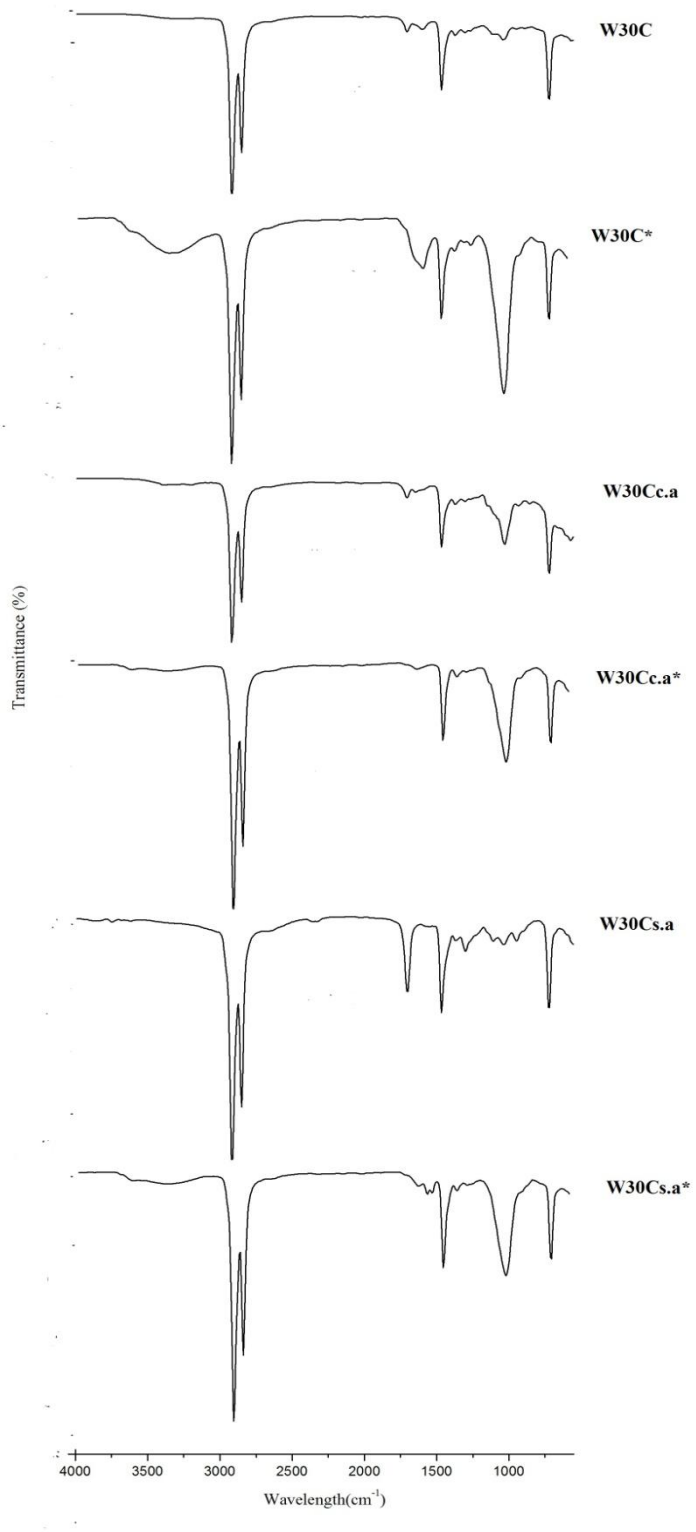

Figure 40: FTIR spectra of the films with 30% TPS loadings from group I before and after soil burial treatment, soil burial notified with star

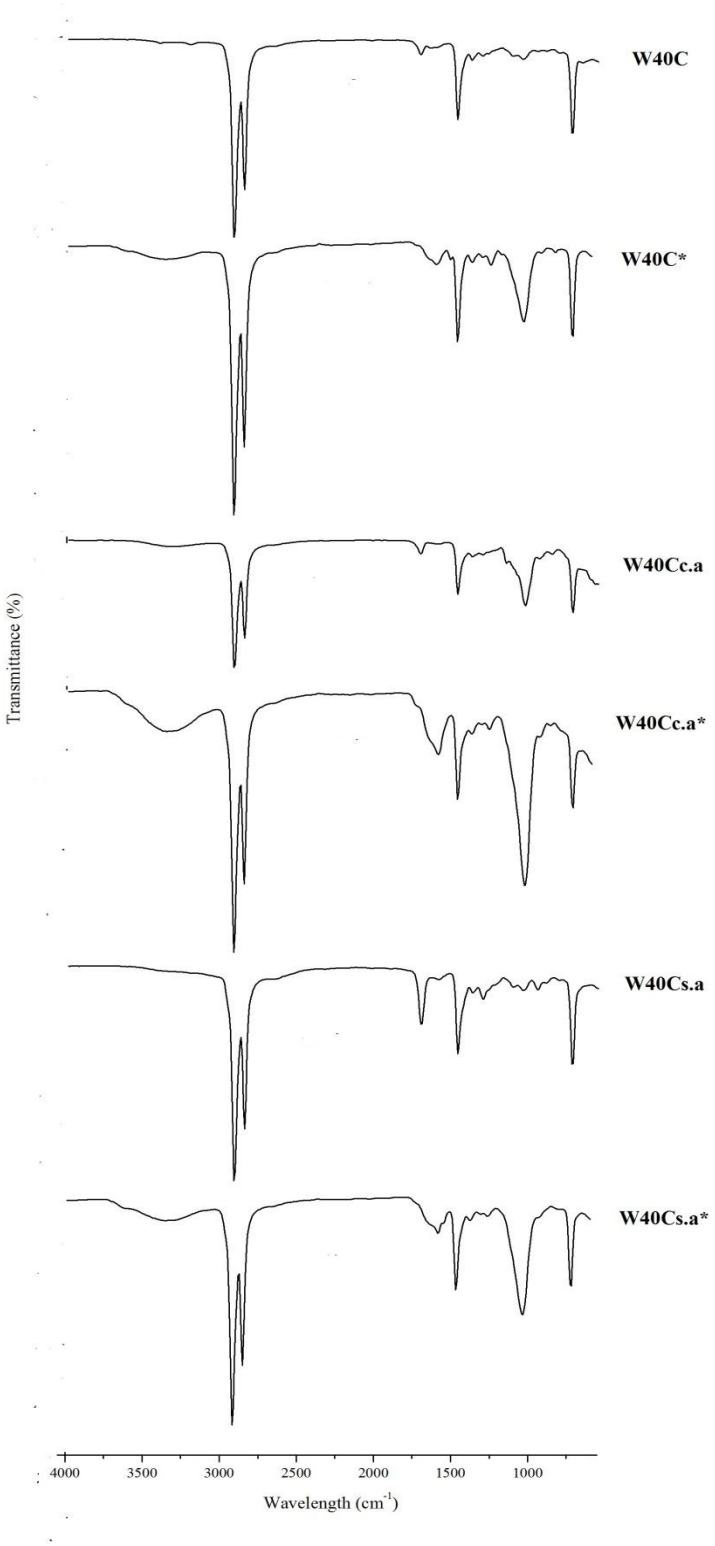

Figure 41: FTIR spectra of the films with 40% TPS loadings from group I before and after soil burial treatment, soil burial notified with star

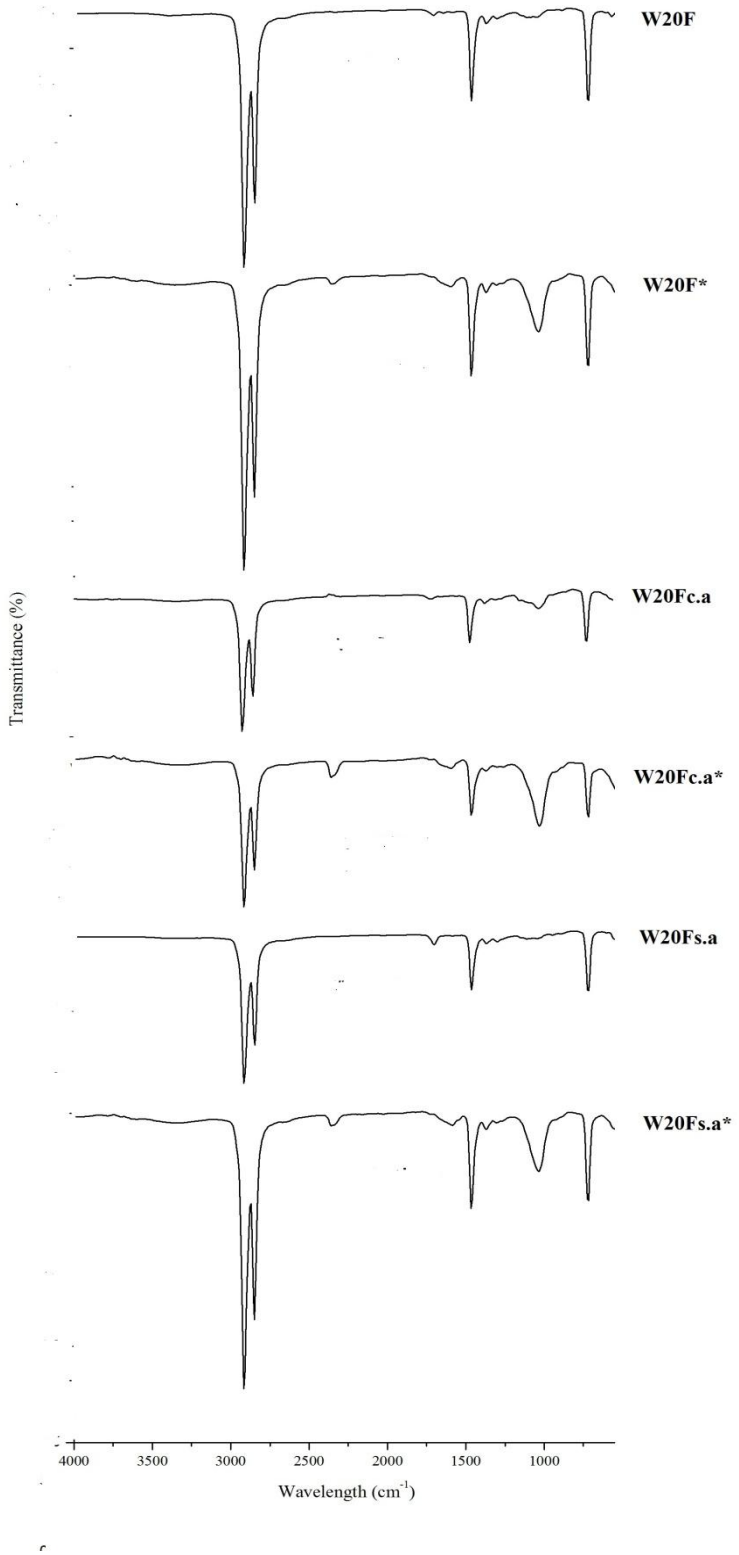

Figure 42: FTIR spectra of the films with 20% TPS loadings from group II before and after soil burial treatment, soil burial notified with star

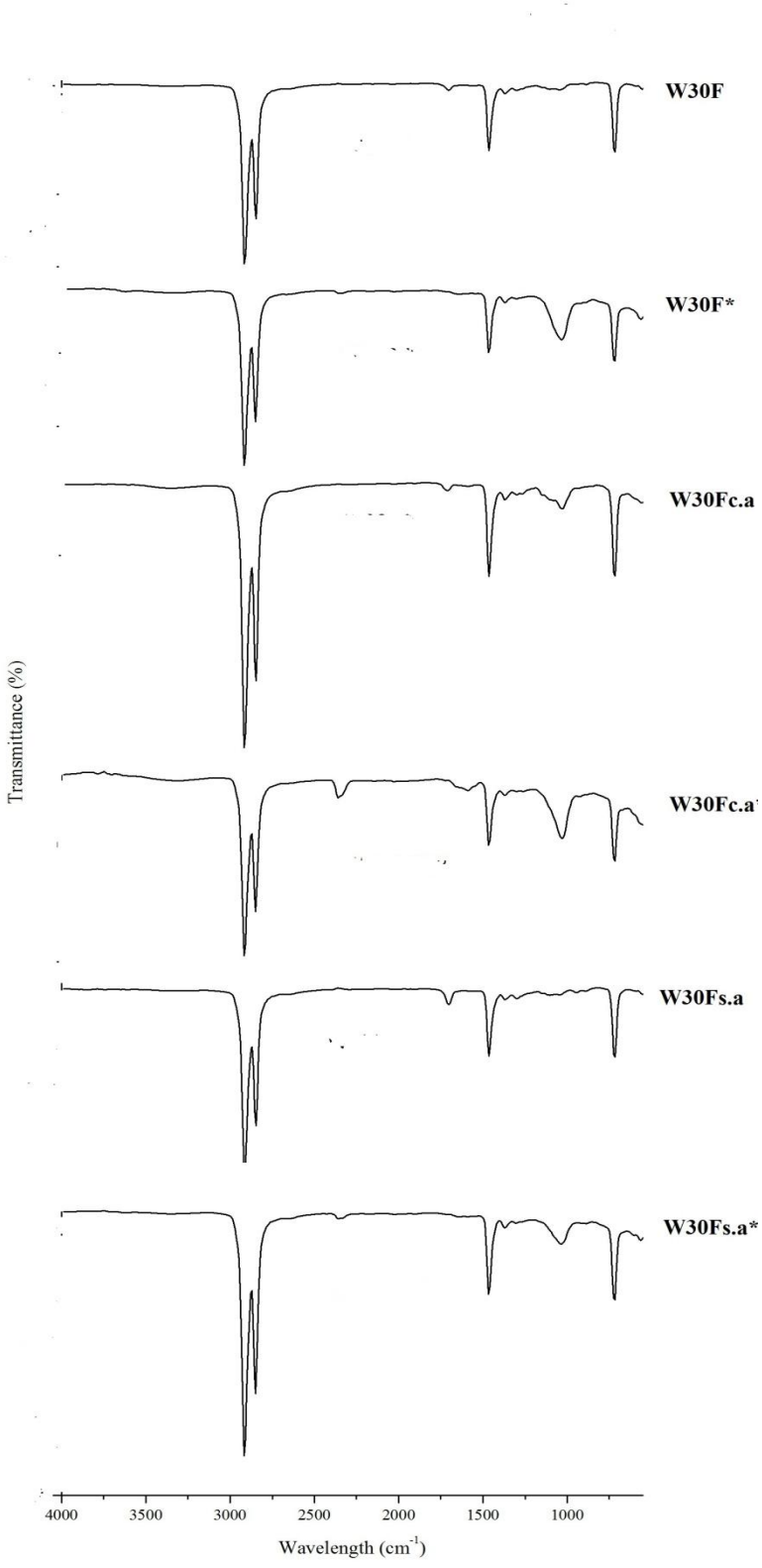

Figure 43: FTIR spectra of the films with 30% TPS loadings from group II before and after soil burial treatment, soil burial notified with star

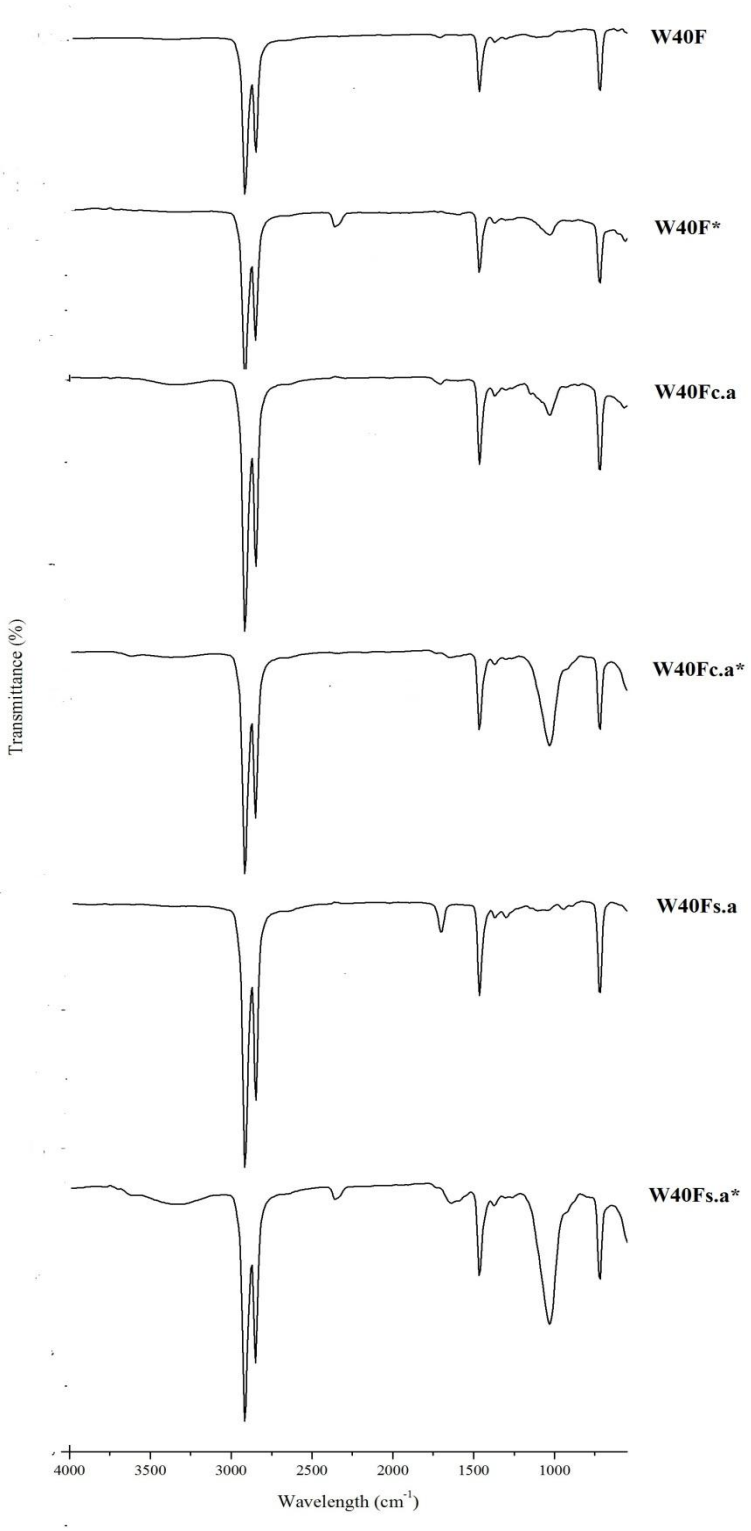

Figure 44: FTIR spectra of the films with 40% TPS loadings from group II before and after soil burial treatment, soil burial notified with star

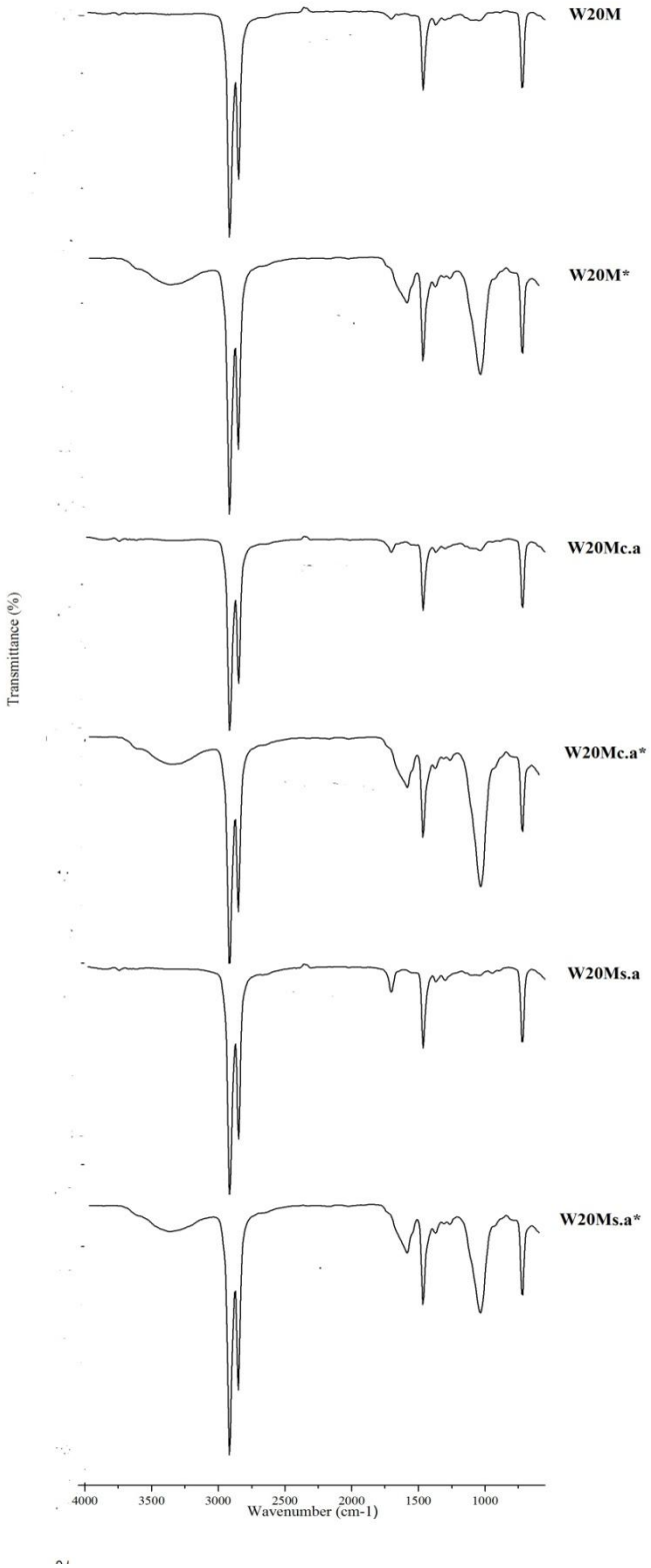

Figure 45: FTIR spectra of the films with 20% TPS loadings from group III before and after soil burial treatment, soil burial notified with star

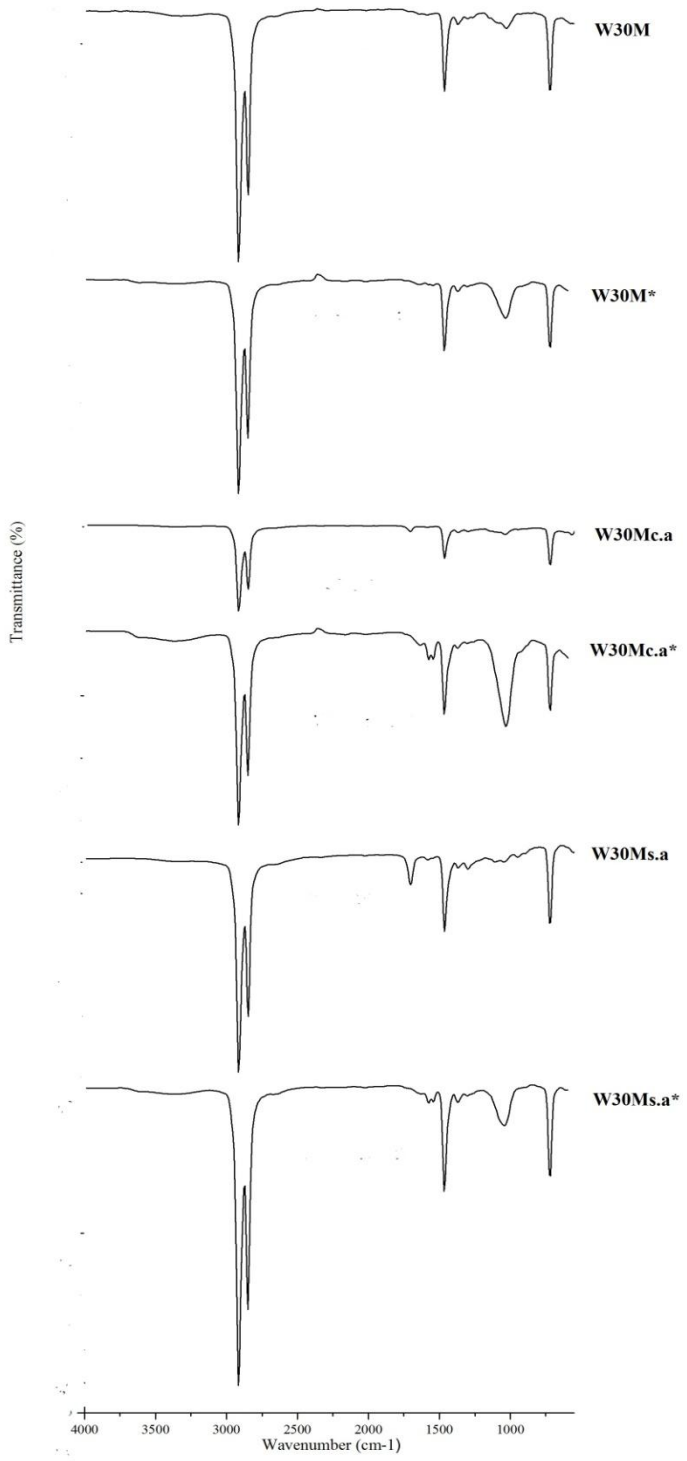

Figure 46: FTIR spectra of the films with 30% TPS loadings from group III before and after soil burial treatment, soil burial notified with star

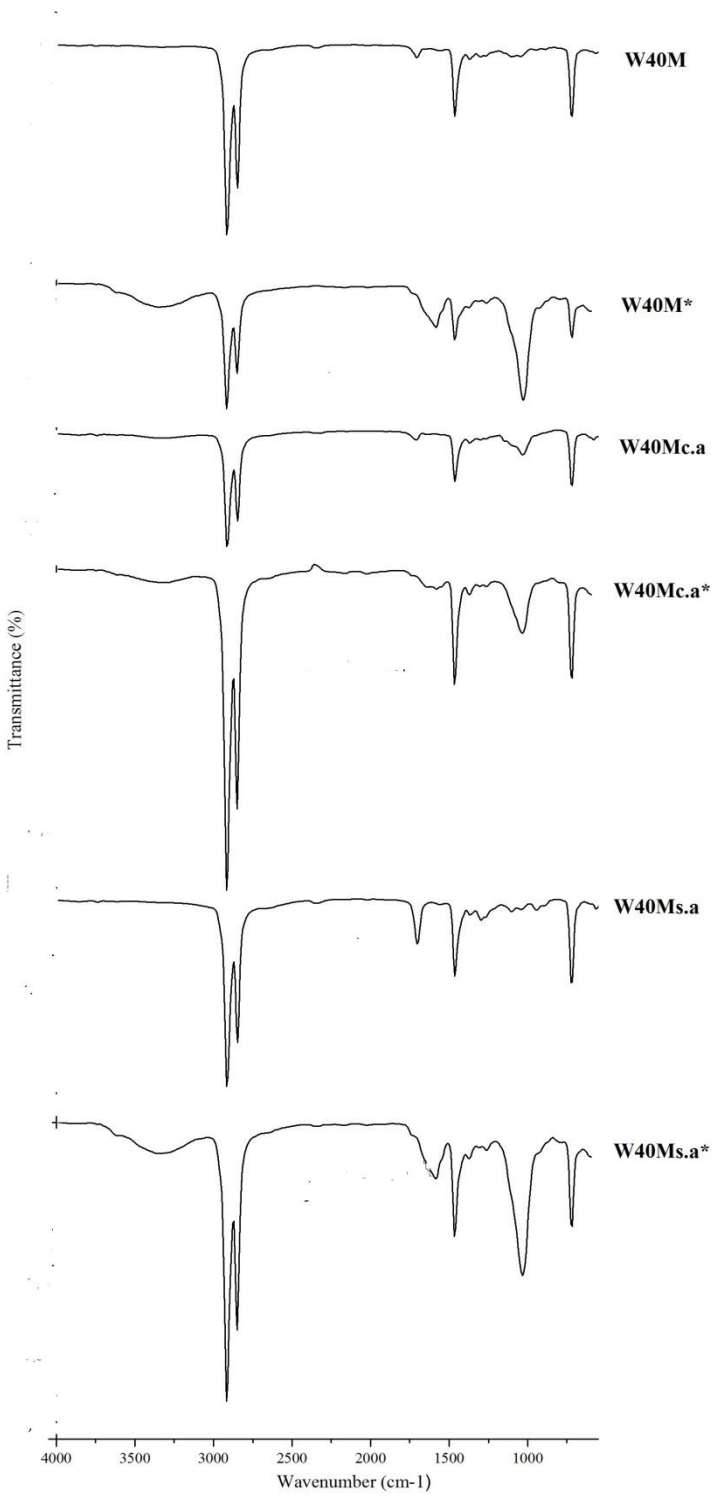

Figure 47: FTIR spectra of the films with 40% TPS loadings from group III before and after soil burial treatment, soil burial notified with star

3.4.3 Thermo -Gravimetric Analysis After Soil Burial Treatment

Thermo-gravimetric analysis was performed for the films, which were exposed to soil environment up to 76 days. TGA curves of these films were plotted in order to understand the degradation.

3.4.3.1. TGA Curves of Group I After Soil Burial Treatment

The TGA curves of the films recovered from soil are displayed Figures 48, 49 and 50. The onset temperatures of the group I before and after burial are tabulated in Table 13.

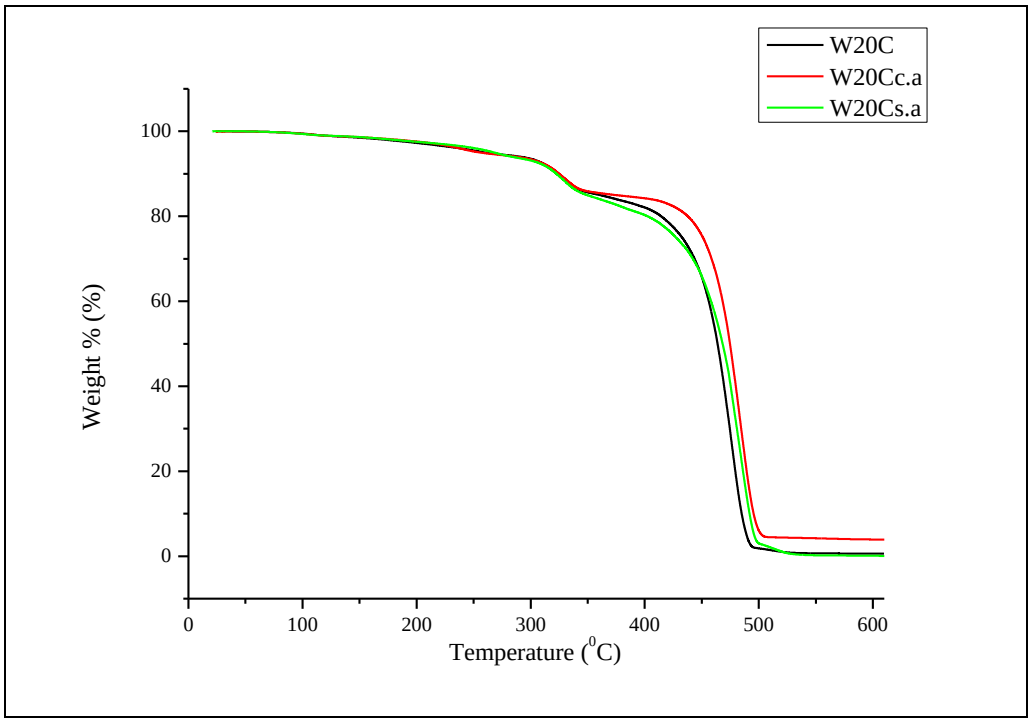

Figure 48: TGA curves of W20C, W20Cc.a and W20Cs.a from group

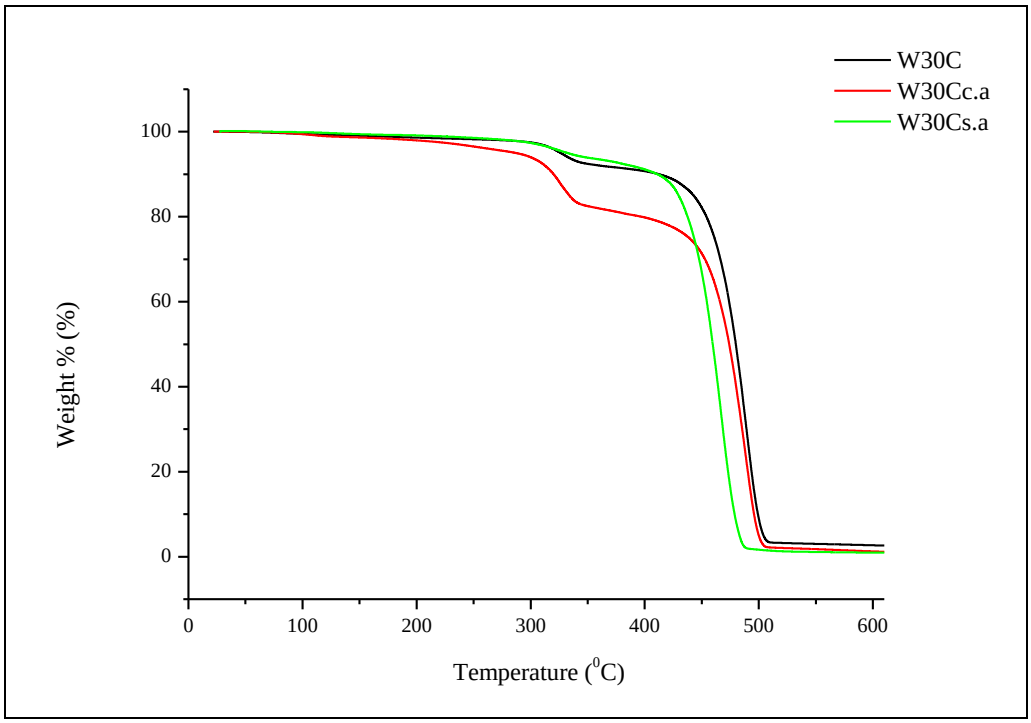

Figure 49: TGA curves of W30C, W30Cc.a and W30Cs.a from group I

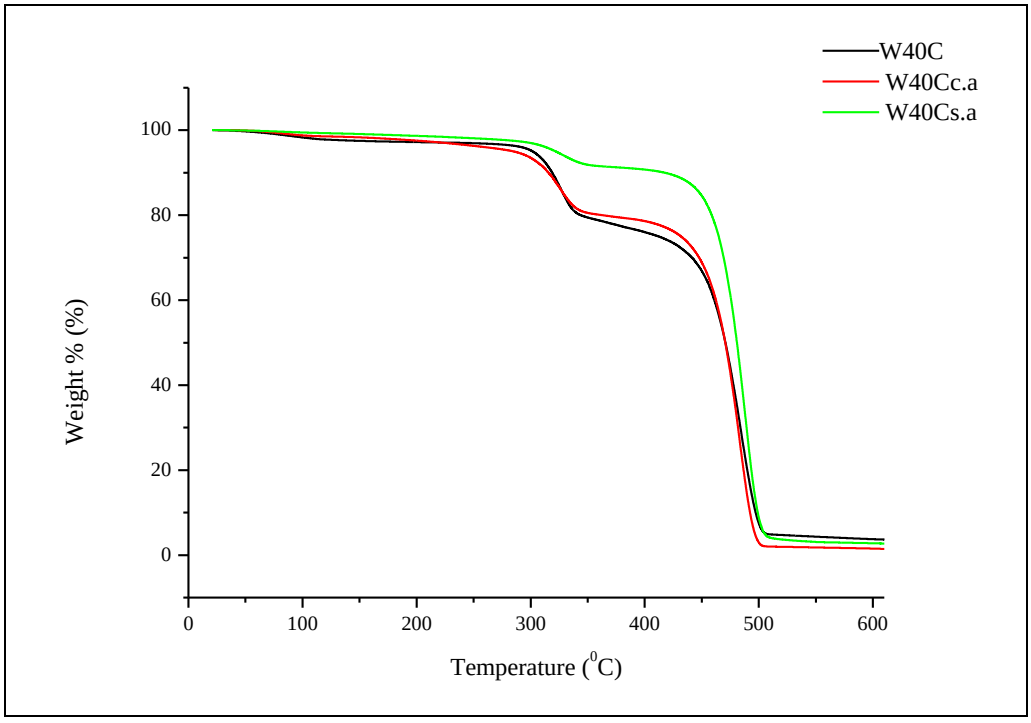

Figure 50: TGA curves of W40C, W40Cc.a and W40Cs.a from group I

Table 13: Decomposition temperatures of group I before and after soil burial treatment

Code of the sample	Evaporation temperature of glycerol (^{0}C)		Degradation temperature of wheat starch (^{0}C)		Degradation temperature of LDPE (^{0}C)	
	Before soil burial	After soil burial	Before soil burial	After soil burial	Before soil burial	After soil burial
W20C	259	-	329	326	482	477
W20Cs.a	240	269	330	329	482	482
W20Cc.a	262	238	328	329	482	482
W30C	255	-	329	326	477	489
W30Cc.a	249	-	331	329	482	486
W30Cs.a	256	-	326	326	471	466
W40C	249	-	328	326	482	484
W40Cc.a	240	-	332	326	481	484
W40Cs.a	254	-	323	328	481	490

As it is displayed in the Figures 50, 51 and 52, the first shift around 100^{0}C was attributed to the loss of water which was absorbed by starch granules. Except the samples coded as W20Cs.a and W20Cc.a, the shift which was attributed to evaporation of glycerol was not observed. It suggests that all the glycerol in the samples except W20Cs.a and W20Cc.a was removed during soil burial treatment.

For films with 30% and 40% TPS, the onset temperatures for the degradation of TPS slightly decreased except the sample coded as W40Cs.a. .When the TGA curves of the films recovered from the soil are compared to the TGA curves of the films before soil burial treatment. It is observed that the weight losses during the shifts attributed to degradation of starch decreased. It was a result of removal of starch by micro organisms.

3.4.3.2. TGA Curves of Group II After Soil Burial Treatment

The TGA curves of the films recovered from soil are displayed Figures 51, 52 and 53. The onset temperatures of the group I before and after burial are tabulated in Table 14.

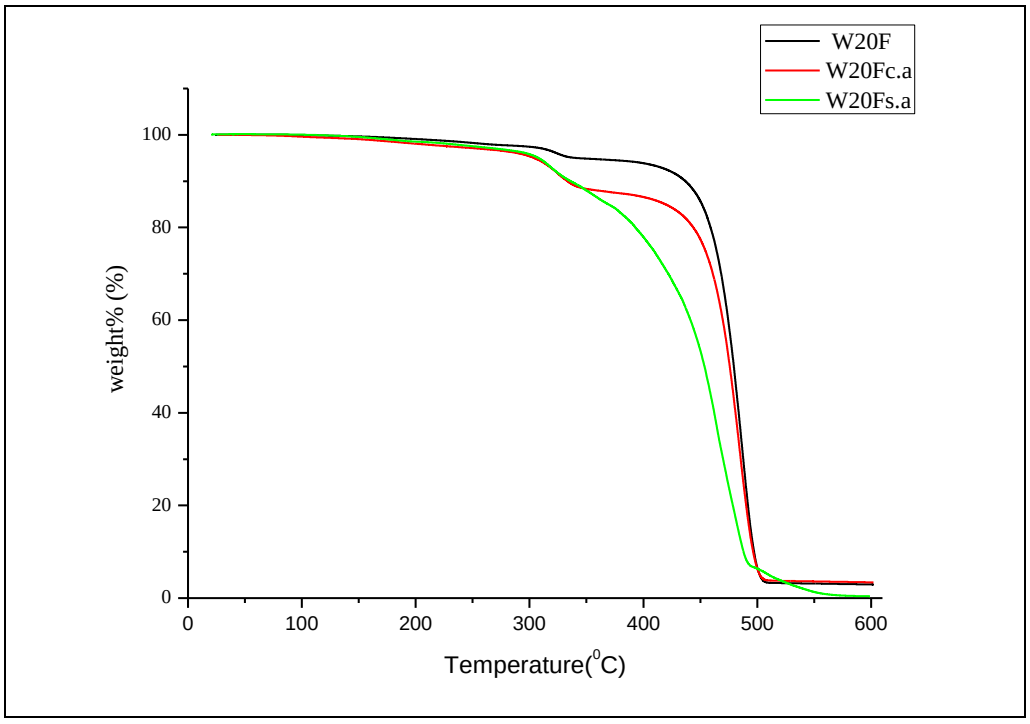

Figure 51: TGA curves of W20F, W20Fc.a and W20Fs.a from group I

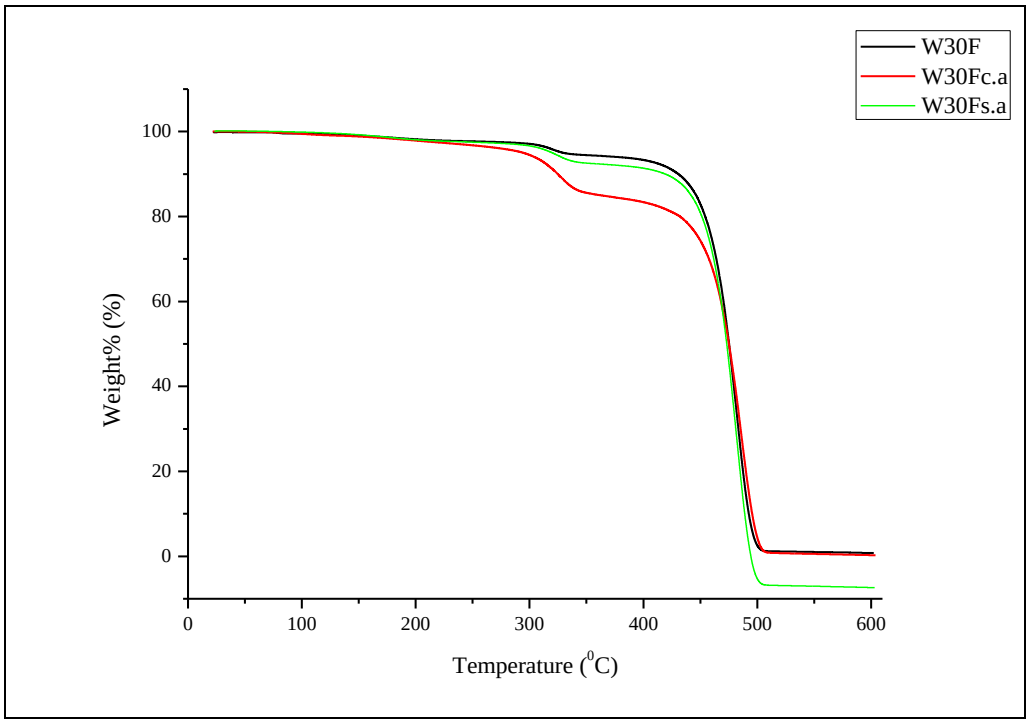

Figure 52: TGA curves of W30F, W30Fc.a and W30Fs.a from group II

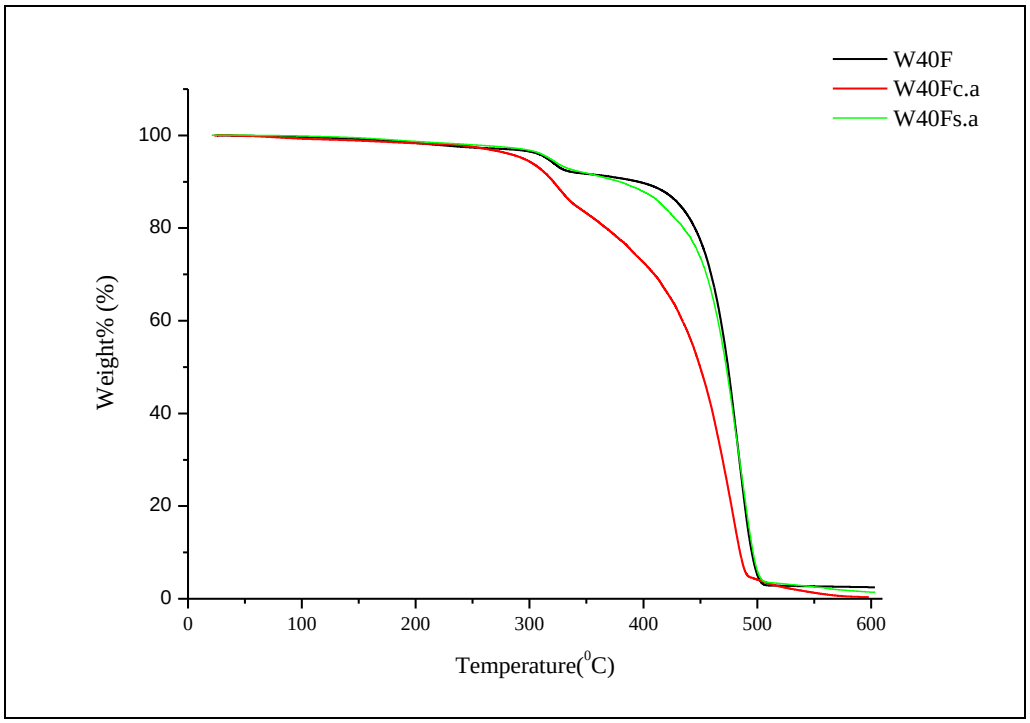

Figure 53: TGA curves of W40F, W40Fc.a and W40Fs.a from group II

Table 14: Decomposition temperatures of group II before and after burial treatment

Code of the sample	Evaporation temperature of glycerol (^{0}C)		Degradation temperature of wheat starch (^{0}C)		Degradation temperature of LDPE (^{0}C)	
	Before soil burial	After soil burial	Before soil burial	After soil burial	Before soil burial	After soil burial
W20F	-	-	315	323	478	486
W20Fc.a	-	-	328	323	479	484
W20Fs.a	-	-	319	319	479	468
W30F	247	-	319	321	479	484
W30Fc.a	242	-	328	326	477	486.
W30Fs.a	247	-	319	326	477	484
W40F	-	-	317	321	475	484
W40Fc.a	249	-	330	324	481	479
W40Fs.a	251	-	321	319	481	484

The shift corresponds to evaporation of glycerol was not observed all through the group II. This indicates that during soil burial the films lost all the glycerol in TPS was removed. No correlation was observed for the blends the onset temperatures before and after soil burial treatment. The degradation temperature of the LDPE mostly increased after the soil burial treatment which was an indication of the loss of glycerol and starch content in the films.

3.4.3.3. TGA Curves of Group III After Soil Burial Treatment

The TGA curves of the films recovered from soil are displayed Figures 54, 55 and 56. The degradation temperatures of group III before and after burial are tabulated in Table 15.

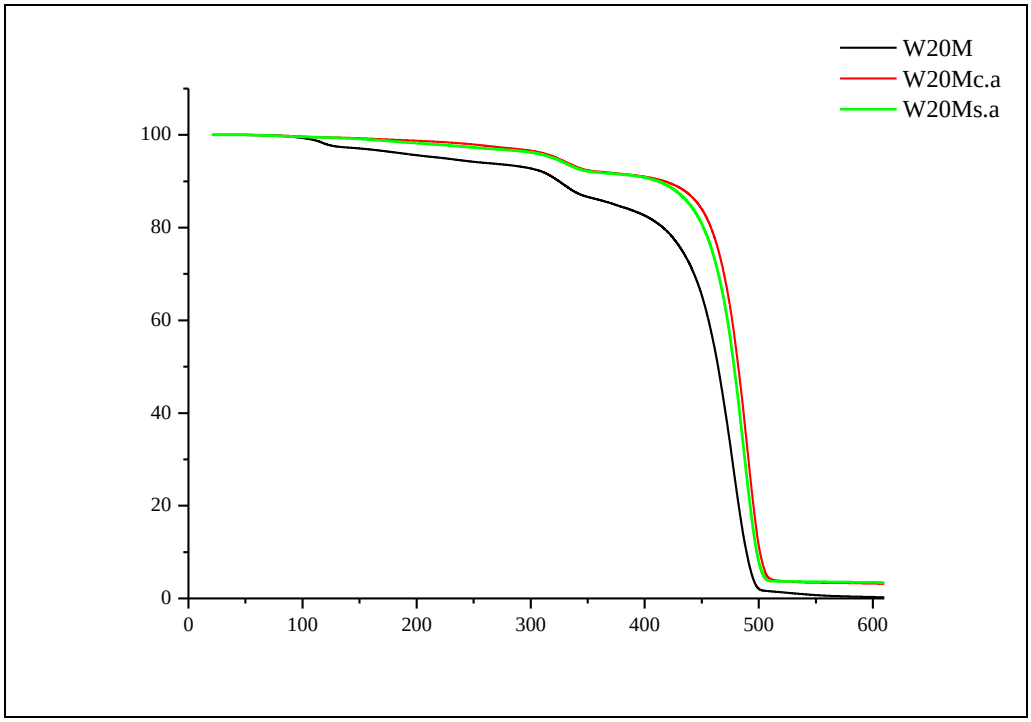

Figure 54: TGA curves of W20M, W20Mc.a and W20Ms.a from group III

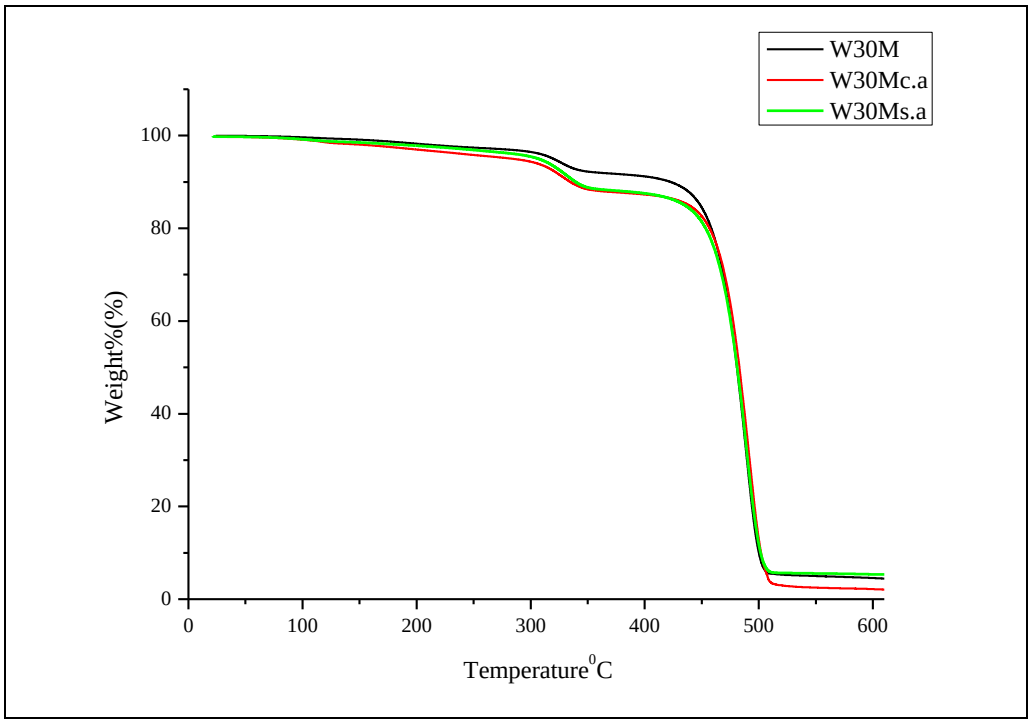

Figure 55: TGA curves of W20M, W20Mc.a and W20Ms.a from group III

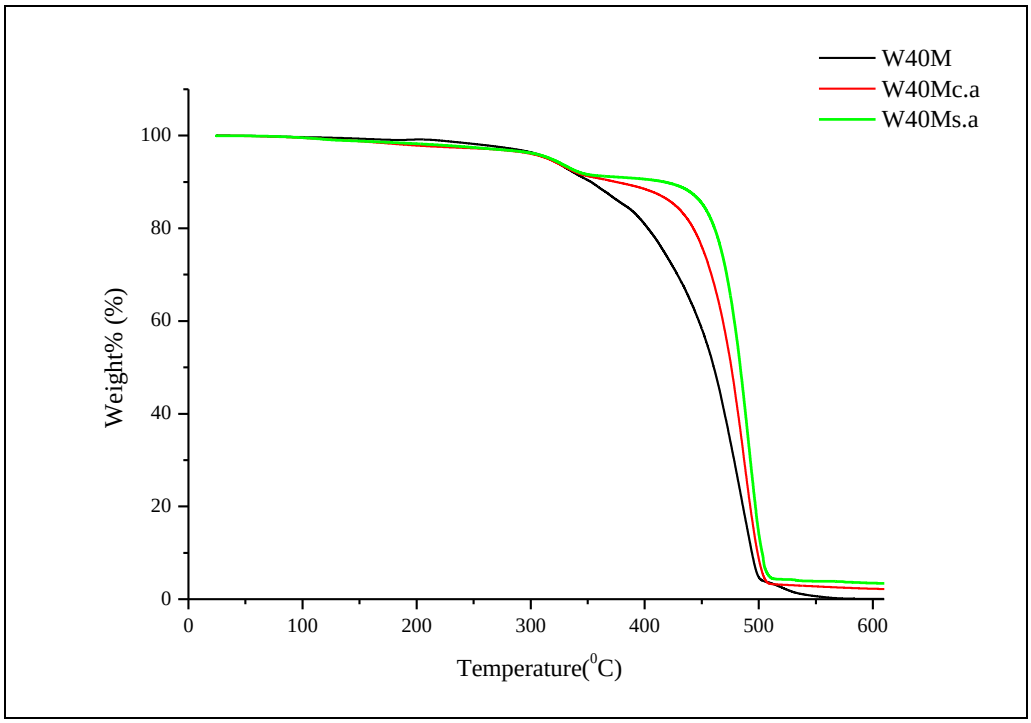

Figure 56: TGA curves of W40M, W40Mc.a and W40Ms.a from group III

Table 15: Decomposition temperatures of group III before and after soil burial treatment

Code of the sample	Evaporation temperature of glycerol		Degradation temperature of wheat starch		Degradation temperature of LDPE	
	Before soil burial	After soil burial	Before soil burial	After soil burial	Before soil burial	After soil burial
W20M	259	-	322	326	481	479
W20Mc.a	246	-	326	330	481	486
W20Ms.a	261	-	324	326	481	490
W30M	258	-	321	328	481	489
W30Mc.a	241	-	326	329	473	490
W30Ms.a	258	-	325	329	481	489
W40M	251	-	321	324	481	486
W40Mc.a	238	-	321	326	481	489
W40Ms.a	254	-	321	326	477	489

There is a slight weight loss at 100^0C through the group, due to the loss of water which was absorbed by starch. The shift attributed to evaporation of glycerol was not seen in all the films in group III, since the glycerol in TPS had been removed during soil burial treatment.

At 20% of TPS loadings, according to weight loss recordings during soil burial treatment agrees with TGA results. The weight loss during soil burial experiment can be attributed to loss of glycerol in TPS; the vast amount of starch was not consumed by micro organisms due to the fact that they were well protected by LDPE and not accessible for the microbial attack.

At higher loadings of starch, 30% and 40%, when the TGA curves of the films recovered from soil are compared to the TGA curves of the films before soil burial treatment, it is observed that the weight losses during the shifts attributed to degradation of starch and removal of glycerol.

3.4.4 Mechanical Properties of the Films After Soil Burial

The mechanical properties of the films from control group, group I, II and III are tabulated in Tables 16, 17, 18 and 19. Due to the loss of integrity, by consumption of the starch, the elongation break values for the control group, group I, II and III dropped dramatically. The tensile strength of the films was not dramatically affected.

Table 16: Mechanical properties of the films from control group after soil burial treatment

Code of the sample	Ultimate tensile strength (MPa)	Elongation at break (%)
W20	9.4	37.2
W30	5.4	34.6
W40	4.0	10.7

Table 17: Mechanical properties of the films from group I after soil burial treatment

Code of the sample	Ultimate tensile strength (MPa)	Elongation at break (%)
W20C	7.4	30.2
W20Cc.a	6.7	42.6
W20Cs.a	9.1	51.9
W30C	6.2	50.7
W30Cc.a	7.7	32.6
W30Cs.a	6.7	23.9
W40C	5.9	69.3
W40Cc.a	6.2	18.7
W40Cs.a	6.4	22.5

Table 18: Mechanical properties of the films from group II after soil burial treatment

Code of the sample	Ultimate Tensile Strength (MPa)	Elongation at Break (%)
W20F	8.1	21.1
W20Fc.a	7.3	92.1
W20Fs.a	8.7	47.2
W30F	6.9	45.6
W30Fc.a	6.6	60.7
W30Fs.a	5.8	21.0
W40F	5.6	21.0
W40Fc.a	6.5	53.6
W40Fs.a	5.7	18.3

Table 19: Mechanical properties of the films from group III after soil burial treatment

Code of the samples	Ultimate Tensile Strength (MPa)	Elongation at Break (%)
W20M	6,1	22.9
W20Mc.a	5,2	33.1
W20Ms.a	7,3	41.0
W30M	4,4	11.6
W30Mc.a	4,7	38.4
W30Ms.a	5,4	39.8
W40M	4,5	8.2
W40Mc.a	4,9	19.5
W40Ms.a	5,2	17.3

CHAPTER 4

CONCLUSION

The studies showed that degradation starts by the consumption of starch when the films were buried in soil without direct exposure to sunlight. During 76 days of burial, LDPE almost did not degrade.

The highest biodegradation rate was observed in the blends with 40% TPS. The film which is coded as W40Cs.a lost 30.99% of its weight after soil burial treatment. Up to 40 days the weight loss was rapid, after it slowed down.

The mechanical properties of the films decreased with increasing starch content. W20Cc.a showed the highest elongation at break, W20C had the highest tensile strength among the blends containing 20% TPS. W30Fc.a showed the highest elongation at break, W30C have the highest tensile strength among the blends containing 30% TPS. W40Cc.a showed the highest elongation at break W40M have the highest tensile strength among the blends containing 30% TPS. After soil burial treatment, percentage elongation break of the films were highly effected, whereas the tensile strength of the films were not affected dramatically.

One of the result of the study was the interaction between compatabilizers and pro-oxidants. When cobalt(II) acetylacetonate used together with citric acid thermal stability of TPS in films were improved. The mechanical properties of the films were also improved. However, it effected biodegradation negatively.

A synergetic effect between iron(III) stearate and citric acid was observed. Using both in the blends resulted in improvement on the thermal stability of TPS in the blends. Significant improvement of the mechanical properties was also observed. The biodegradation rates were slightly improved as a result of using of this two chemicals in the blend.

Moreover,when manganese(II) stearate used together with citric acid, a decrease in the mechanical properties was observed compared to the blends with both manganese(II) stearate and stearic acid. However, a significant improvement was not observed in terms of thermal stability of TPS in the blends.

Another observation is that regardless of the pro-oxidant used, TGA curves of the films showed that addition of citric acid decrease the interaction between starch and glycerol, resulting in lower temperatures of evaporation of glycerol.

Finally, under these conditions studies showed that the films with 40% of TPS in group I can be good candidates for mulch films in terms of their optimized biodegradation rates and mechanical properties.

REFERENCES

[1] Leejarkpai T., Suwanmanee U., Rudeekit Y., Mungcharoen T., *Biodegradable kinetics of plastics under controlled composting conditions.* Waste Management vol.31, 1153–1161, (2010).

[2] Hamid H.., Amin B.M., Maadhah A.G.,*Handbook of Polymer Degradation*, Marcel Dekker , Inc.,New York, (1992).

[3] Lucy S. Vlietstra S.L, Parga J.A., *Long-term changes in the type, but not amount, of in gested plasticparticles in short-tailed shearwaters in the southeastern Bering Sea,* Marine Pollution Bulletin,vol.44, 945-955, (2002).

[4] Kapanen A., Schettini E., Vox G., Itaavaara M., *Performance and Environmental Impact of Biodegradable Films in Agriculture: A Field Study on Protected Cultivation, Journal of the Polymers and the Environment*, vol.16, 109–122, (2008).

[5] Retrieved on September 12, 2012 from http://www.greenhouseworld.com/clear-poly-row-cov 1000_03D07_product.html.

[6] Retrieved on September 12, 2012 from http://www.buzzle.com/articles/how-to-use-a-greenhouse.html.

[7] Retrieved on September 12, 2012 from http://www.alibaba.com/product-gs/249743476/Agricultural_Mulching_Film.html.

[8] Retrieved on September 12, 2012 from http://safarnoori.blogspot.com /2011/05/ mulching-for-weed-control-iannual.html.

[9] Scott G., Gilead D., *Degradable polymers*, Champan&Hall, London, (1995).

[10] Gupta A. P., Kumar V., Sharma M., *Formulation and Characterization of Biodegradable Packaging Film Derived from Potato Starch & LDPE Grafted with Maleic Anhydride—LDPE Composition,* Journal of Polymer and Environment , vol. 18, 484–491, (2010).

[11] Rosato D.V.,. Schott N. R. , Rosato M. G., *Plastics Engineering, Manufacturing & Data Handbook,* Kluwer Acedemic Publishers,USA.

[12] Arutchelvi J., Sudhakar M., Arkatkar A.,*Biodegradation of polyethylene and polypropylene, Polymer Degradation and Stability,* vol 95, 1011-10, (2007).

[13] Ranby B., Rabek J.F, *Photodegradation, Photo oxidation and Photostabilization of Polymers, A wiley –Interscience Publication*, England, (1975).

[14] Koutny M., Lemaire J., Delort A., *Biodegradation of polyethylene films with prooxidant additives,* Chemosphere vol 64 , 1243–1252, (2006).

[15] Moeller W.H, *Progress in polymer degradation and stability research*, Nova Science Publishers,Inc., New york, (2008).

[16] Kim M., *Evaluation of degradability of hydroxypropylated potato starch/polyethylene blend films*, Carbohydrate Polymer, vol. 54, 173–181, (2003).

[17] Gupta A. P., Kumar V., Sharma M., and Shukla S. K. , *Physicochemical Studies on Interaction Behavior of Potato Starch Filled Low Density Polyethylene Grafted Maleic Anhydride and Low Density Polyethylene Biodegradable Composite Sheets, Polymer-Plastics Technology and Engineering*, vol. 48, 587–594, (2009).

[18] Chiellini E., Cinelli P., Chiellini F., Imam H. S, *Environmentally Degradable Bio-Based Polymeric Blends and Composites*, Macromolecular bioscience,vol.4, 218 -231,(2004).

[19] Gupta P. , Sharma M. , Kumar V., *Preparation and Characterization of Potato Starch Based Low Density Polyethylene/Low Density Polyethylene Grafted Maleic Anhydride Biodegradable Polymer Composite,* Polymer-Plastics Technology and Engineering, vol .47, 953–959, (2008).

[20] Retrieved on September 12, 2012 from http://www.lsbu.ac.uk/water/hysta.html.

[21] Retrieved on September 12, 2012 from http://www.rsc.org/Education/Teachers/Resources/cfb/carbohydrates.html.

[22] Zhang Y., Rempel C., *Retrogradation and Antiplasticization of Thermoplastic Starch , Richardson Centre for Functional Foods and Nutraceuticals*.

[23] Prachayawarakorn J. , Sangnitidej P.,Boonpasith P., *Properties of thermoplastic rice starch composites reinforced by cotton fiber or low-density polyethylene, Carbohydrate Polymers* , vol.81, 425–433, (2010).

[24] Da Róz A.L. ,Carvalho A.J.F., Gandini A., Curvelo A.A.S.,*The effect of plactizers on thermoplastic starch comositions obtained my melt processing*, Carbohydrate Polymers vol 63, 417–424, (2006).

[25] Tena-Salcido C. S. , Rodríguez-González F. J. , Méndez-Hernández M. L. , Contreras-Esquivel J.C., *Effect of Morphology on the Biodegradation of Thermoplastic Starch in LDPE/TPS Blends*,Polymer Bulletin,vol.60, 677–688 (2008).

[26] Ning W., Jiugao Y., Xiaofei M., Ying W. *The influence of citric acid on the properties of thermoplastic starch/linear low-density polyethylene blends*,Carbohydrate Polymers 67,446–453, (2007).

[27] Thakore I.M, Desai S., Sarawade B.D., Devi S., *Studies on biodegradability, morphology and thermomechanical properties of LDPE/modified starch blends,* European Polymer Journal vol.37 ,150-160, (2001).

[28] Retrieved on September 12, 2012 from http://www.chemistryland.com/CHM151W/04Solutions/acids/AcidsBases151.html

[29] Retrieved on September 12, 2012 from http://sci-toys.com/ingredients/stearic_acid.html

[30] Abd El-Rehim H.A, Hegazy E.A, Ali A.M, Rabie A.M. ,*Synergistic effect of combining UV-sunlight–soil burial treatment on the biodegradation rate of LDPE/starch blends,* Journal of Photochemistry and Photobiology A: Chemistry, vol.163, 547–556, (2004).

[31] Sharma N., Chang L.P. Chu Y.L., Ismail H. , Ishiaku U.S., Mohd Ishak Z.A, A study on the effect of pro-oxidant on the thermo-oxidative degradation behaviour of sago starch filled polyethylene, Polymer Degradation and Stability, vol. 71, 381±39,(2001).

[32] Retrieved on September 12, 2012 from http://www.chemicalbook.com/ ChemicalProductProperty_EN_CB1353969.htm.

[33] Retrieved on September 12, 2012 from http://www.chemicalbook.com/ ChemicalProductProperty_EN_CB8137795.htm.

[34] Retrieved on September 12, 2012 from http://www.chemicalbook.com/ ChemicalProductProperty_EN_CB6220394.htm.

[35] Ruiz H.V, Martinez E.S.M, Mendez M.M.A., *Biodegradability of polyethylene–starch blends prepared by extrusion and molded by injection: Evaluated by response surface methodology,* Starch/Starke 2011, vol.63, 42–51, (2010).

[36] Baldev R. K. Udaya Sankar K.,*LDPE/Starch blend films for food packaging applications* Advances in Polymer Technology, vol. 23, No. 1, 32–45, (2004).

[37] Peanasky J. *S.* , Long J. M., Wool R. P. *Percolation Effects in Degradable Polyethylene-Starch Blends,* (1990).

APPENDIX A

Weight recordings for the samples

Table 20: Weight loss recordings for control group

Code	Weights of the samples (g)		
	Day 0	Day 40	Day 76
W20	0,6757	0,6843	0,6755
W30	0,6963	0,6683	0,6503
W40	0,8088	0,7418	0,7105

Table 21: Weight loss recordings for group I

Code	Weights of the samples (g)		
	Day 0	Day 40	Day76
W20C	0,6035	0,5997	0,5877
W20Cc.a	0,5311	0,5293	0,5112
W20Cs.a	0,5760	0,5658	0,5618
W30C	0,6501	0,5387	0,5123
W30Cc.a	0,7752	0,7359	0,7168
W30Cs.a	0,6179	0,5236	0,5029
W40C	0,8092	0,6631	0,6415
W40Cc.a	0,5731	0,4862	0,4762
W40Cs.a	0,7187	0,5063	0,4964

Table 22: Weight loss recordings for group II

Code	Weights of the samples (g)		
	Day 0	Day 40	Day76
W20F	0,7992	0,8099	0,7876
W20Fc.a	0,7736	0,7367	0,6708
W20Fs.a	0,6847	0,6792	0,6604
W30F	0,7504	0,7368	0,7074
W30Fc.a	0,8285	0,7898	0,7122
W30Fs.a	0,5387	0,4928	0,4760
W40F	0,7759	0,7048	0,6821
W40Fc.a	0,6126	0,5004	0,4900
W40Fs.a	0,7694	0,6289	0,6092

Table 23: Weight loss recordings for group III

Code	Weights of the samples (g)		
	Day 0	Day 40	Day76
W20M	0,6495	0,6468	0,6433
W20Mc.a	0,5413	0,5307	0,5147
W20Ms.a	0,4362	0,4191	0,4116
W30M	0,7360	0,6931	0,6797
W30Mc.a	0,6671	0,6096	0,5810
W30Ms.a	0,7967	0,7596	0,7287
W40M	0,6767	0,5687	0,5428
W40Mc.a	0,7128	0,5714	0,5538
W40Ms.a	0,6316	0,5505	0,5309